

1 **Detecting Methane Ebullition on Thermokarst Lake Ice**
2 **Using High Resolution Optical Aerial Imagery**

3

4 **P. R. Lindgren¹, G. Grosse^{2,1}, K. M. Walter Anthony³, F. J. Meyer¹**

5 [1] Geophysical Institute, University of Alaska Fairbanks, USA

6 [2] Alfred Wegener Institute Helmholtz Centre for Polar and Marine Research, Potsdam,
7 Germany

8 [3] Water and Environmental Research Center, University of Alaska Fairbanks

9 Correspondence to: P. R. Lindgren (pregmi@alaska.edu)

10

11

12

13

14

15

16

17

18

19

20

21

22

23

24

25

Résumé des commentaires sur
PRLindgren_et_al_2015_BGD_MANUSCRIPT

Cette page ne contient aucun commentaire.






1 Abstract

2 Thermokarst lakes are important emitters of methane, a potent greenhouse gas. However,
3 accurate estimation of methane flux from thermokarst lakes is difficult due to their
4 remoteness and observational challenges associated with the heterogeneous nature of
5 ebullition¹ (bubbling). We used multi-temporal high-resolution (9 -11 cm) aerial images of an
6 interior Alaskan thermokarst lake, Goldstream Lake, acquired 2 and 4 days following freeze-
7 up in 2011 and 2012, respectively, to characterize methane ebullition seeps and to estimate
8 whole-lake ebullition.² Bubbles impeded by the lake ice sheet form distinct white patches as a
9 function of bubbling rate versus time as ice thickens. Our aerial imagery thus captured in a
10 single snapshot the ebullition events that occurred before the image acquisition. Image
11 analysis showed that low-flux A- and B-type seeps are associated with low brightness patches
12 and are statistically distinct from high-flux C-type and Hotspot seeps associated with high
13 brightness patches. Mean whole-lake ebullition based on optical image analysis in
14 combination with bubble-trap flux measurements was estimated to be $174 \pm 28 \text{ ml gas m}^{-2} \text{ d}^{-1}$
15 and $216 \pm 33 \text{ ml gas m}^{-2} \text{ d}^{-1}$ for the years 2011 and 2012, respectively. A large number of
16 seeps demonstrated spatio-temporal stability over³ our two-year study period. A strong inverse
17 exponential relationship ($R^2 \geq 0.79$) was found between percent surface area of lake ice
18 covered with bubble patches and distance from the active thermokarst lake margin. Our study
19 shows that optical remote sensing is a powerful tool to map ebullition seeps on lake ice, to
20 identify their relative strength of ebullition and to assess their spatio-temporal variability.

21

22 1 Introduction

23 Soils in the northern permafrost region contain 1300-1370 Pg of organic carbon with an
24 uncertainty range of 930-1690 Pg (Hugelius et al., 2014). A large amount of soil carbon in the
25 Yedoma permafrost region (~450 Pg) is found⁴ in thick Holocene deposits in thermokarst lakes
26 and basins, Pleistocene-age ice-rich silts known as yedoma, and Pleistocene deposits thawed
27 underneath lakes (Grosse et al., 2011; Walter Anthony et al., 2014).⁵ However, permafrost
28 degradation can facilitate the transfer of this permafrost stored carbon to the atmosphere in the
29 form of the greenhouse gases carbon dioxide (CO₂) and methane (CH₄), resulting in a positive
30 feedback to global climate change (Zimov et al., 2006; Walter et al., 2006; Schuur et al.,
31 2008; Koven et al., 2011). One common and effective form of permafrost degradation
32 involves formation and growth of thermokarst lakes (Grosse et al., 2013; Kokelj and

 Nombre : 1	Auteur :	Sujet : Commentaire sur le texte	Date : 2015-10-28 11:40:00
is this necessary?			
 Nombre : 2	Auteur :	Sujet : Commentaire sur le texte	Date : 2015-10-28 14:33:27
This is unclear (because you are using both "as a function" and "versus" and "as" in the same sentence!). And why "versus time" if the image is a snap shot in time?			
 Nombre : 3	Auteur :	Sujet : Commentaire sur le texte	Date : 2015-10-28 11:50:54
replace by "this"?			
 Nombre : 4	Auteur :	Sujet : Commentaire sur le texte	Date : 2015-10-28 12:11:39
why the distinction between the last 2?			
 Nombre : 5	Auteur :	Sujet : Commentaire sur le texte	Date : 2015-10-28 12:13:22
why "however"?			

1 Jorgenson, 2013), which tap into deep (up to 60m) permafrost carbon pools (Zimov et al.,
2 1997; Walter et al., 2008a).

3 Thermokarst lakes are a prominent landscape feature in the high northern latitudes (Smith et
4 al., 2007; Grosse et al., 2013). They are formed in closed depressions following the thawing
5 of ice-rich permafrost or melting of massive ice. Once initiated, the presence of a water body
6 on permafrost serves as a positive feedback to permafrost degradation. Depending on the
7 amount of excess ice content in permafrost, this positive feedback accelerates the growth of
8 thermokarst lakes in both lateral and vertical directions (Jorgenson and Shur, 2007; Plug and
9 West, 2009; Kokelj and Jorgenson, 2013). Over many years, taliks (thaw bulbs) of perennially
10 thawed soil develop beneath thermokarst lakes (Hinzman et al., 2005; West and Plug, 2008;
11 Rowland et al., 2011) creating conditions favorable for year-round methane production
12 through anaerobic decomposition of organic matter by microbes (Zimov et al., 1997; Walter
13 et al., 2006, 2008a; Kessler et al., 2012). During lateral expansion, thermal erosion along the
14 lake margin also releases both Holocene and Pleistocene organic matter from adjacent soils
15 into anaerobic lake bottoms further enhancing methanogenesis (Zimov et al., 1997; Walter
16 Anthony et al., 2014).

17 Ebullition (bubbling) is considered the dominant pathway of methane release from lakes to
18 the atmosphere (Keller and Stallard, 1994; Bastviken et al., 2011). Methane produced in
19 dense lake sediments and thaw bulbs emerges primarily through intrasedimentary bubble
20 tubes as point-source seeps on the lake bed (Walter Anthony et al., 2010). In the high northern
21 latitude region, where lake surfaces freeze throughout the winter, most bubbles emerging
22 from the lake bed ascend through the water column and get trapped by ice as gas-pockets
23 (Walter et al., 2008b; Greene et al., 2014). Ongoing ice growth can separate ice-trapped
24 bubbles from an individual seep by thin films of ice, resulting in vertically oriented bubble
25 columns in the ice. Walter et al. (2006) took advantage of this phenomenon to reveal locations
26 and relative strength of “point-sources” of methane seep ebullition across lake ice. They
27 identified four major types of methane ebullition seeps based on ice bubble cluster
28 morphology and they measured daily mean ebullition rates (Fig. 1) (Walter Anthony and
29 Anthony, 2013). It should be noted that seep class-specific ebullition rates reported represent
30 the daily average of thousands of flux measurements; however, bubbling within each class is
31 highly episodic, and bubbling rates of individual seeps are not constant over time (Walter
32 Anthony et al., 2010; Walter Anthony and Anthony, 2013): (1) A-type seeps are characterized

1 by isolated bubbles stacked in multiple vertical layers with less than 50% of all gas volume
2 merged in bubble clusters. A-type seeps have the lowest ebullition rate (22 ± 4 ml gas d⁻¹); (2)
3 B-type seeps are dominated by laterally-merged bubbles stacked in multiple layers (more than
4 50% of all gas volume merged in a bubble cluster). The ebullition rate of this bubble type is
5 211 ± 39 ml gas d⁻¹; (3) C-type seeps, associated with an ebullition rate of 1726 ± 685 ml gas
6 d⁻¹, are characterized by single large gas pockets (usually > 40 cm in diameter) separated
7 vertically by ice layers containing few or no bubbles; and (4) Hotspot seeps have the highest
8 ebullition rate, on average 7801 ± 764 ml gas d⁻¹. Due to upwelling of water associated with
9 frequent bubble streams, Hotspots generally appear as open-water holes in lake ice following
10 freeze up. Usually a thin snow-ice film develops over Hotspots in winter, visually masking
11 them at the surface; however, ice blocks cut from the lake throughout winter and spring reveal
12 that Hotspot bubbling maintains a large ice-free cavity throughout winter (Greene et al.,
13 2014).

14 Accounting for methane ebullition from northern thermokarst lakes can significantly improve
15 estimates of lake contributions to regional and global atmospheric carbon budgets (Walter et
16 al., 2007; Bastviken et al., 2011). However, due to challenges associated with the logistics of
17 fieldwork in remote locations as well as spatial and temporal heterogeneity of ebullition,
18 accurate estimation of methane flux from thermokarst lakes is difficult (Casper et al., 2000;
19 Bastviken et al. 2004; Wik et al., 2011). Most studies have been carried out using field
20 measurements to understand the spatial and temporal variability of methane ebullition.
21 However, insufficient field data is a recurring issue since it is difficult to sample the entire
22 lake area, particularly when lakes have remote locations. This may lead to an unrealistic
23 characterization of ²variability of ebullition bubbles and a less accurate estimation of methane
24 flux at a regional scale. Recently, Walter Anthony and Anthony (2013) combined point-
25 process modeling with field-measured data to understand the drivers of ebullition spatial
26 variability in thermokarst lakes and provided ways to reduce uncertainty in regional-scale lake
27 ebullition estimates based on limited field data; nonetheless spatially-limited field sampling
28 remains a hindrance to whole-lake ebullition quantification .

29 Remote sensing methods combined with field observations can help overcome some of the
30 limitations that exist in a sole field-survey method. One of the major advantages of remote
31 sensing tools is that they may provide the possibility to map the entire population of methane
32 ebullition bubbles on a lake. Moreover, remote sensing can overcome the logistical

1 Nombre : 1 Auteur : Sujet : Commentaire sur le texte Date : 2015-10-28 14:35:09

this standard deviation (and the other below for other types) corresponds to which data set? How many lakes? How many measurements? over what region? for what type of permafrost and sediment deposits? This is not a generality

1 Nombre : 2 Auteur : Sujet : Commentaire sur le texte Date : 2015-10-28 14:36:07


I suggest to replace "variability of ebullition bubbles" by "whole-lake ebullition" to clarify this sentence.

And just an idea to make the text lighter: "ebullition bubble" seems a redundant expression, which is repeated at several occasions throughout the paper. I understand that bubbles formed by ice exclusion of gases are not coming from sediment ebullition, but is this the only reason why you keep using this expression throughout? I think readers can understand that when you talk about bubbles, you are referring to ebullition bubbles.


1 difficulties that exist in accessing methane-bubbling lakes in the remote regions of the Arctic
2 and Subarctic. Previously, scientists who used remotely sensed images from synthetic
3 aperture radar (SAR) sensors to study lake ice phenology detected tiny (1-5 mm diameter)
4 vertically-oriented tubular gas bubbles trapped in ice that form when dissolved gases are
5 excluded during ice formation (Jeffries et al., 1994; Jeffries et al., 2005; Duguay et al., 2003).
6 The presence of these sometimes densely-packed non-ebullition gas bubbles, which are
7 usually ubiquitous across the lake if they occur in the ice at all (Boereboom et al., 2012), can
8 have significant effect on spectral and SAR backscatter properties of lake ice, ¹particularly in
9 late winter and spring when dissolved gas concentrations in lake water are highest (Phelps et
10 al., 1998; Langer et al., 2014). In contrast, individual ebullition bubbles, which are larger (0.5-
11 3 cm) (Walter Anthony et al., 2010; Langer et al., 2014) and tend to cluster together (cluster
12 diameter usually 5 to >100 cm), ²are also detected with remote-sensing SAR sensors (Engram
13 et al., 2012). Walter et al. (2008b) and Engram et al. (2012) demonstrated the potential
14 application of SAR satellite imagery to estimate whole-lake ebullition from spatially-limited
15 field measurements of ebullition along survey transects. These studies showed correlation of
16 radar backscatter values with the percent surface area of lake ice covered with bubbles and
17 field-measured methane ebullition rates based on bubble-trap measurements from lakes.
18 Additionally, Walter Anthony et al. (2012) used aerial surveys to identify, ³photograph, and
19 map large (~1 m² to > 300 m²) bubbling-induced open-water holes in ice-covered lakes in
20 Alaska associated with geologic methane seepage. Coupling aerial surveys with ground truth
21 flux measurements and laboratory analyses, this study showed that geologic methane seepage
22 is not extensive, but it is important in some regions of Alaska underlain by leaky hydrocarbon
23 reservoirs.

24 Since open holes in lake ice induced by bubbling are visually distinct, and since lower-flux
25 ebullition bubble clusters trapped inside ice appear as bright white features that have a strong
26 contrast against dark, bubble-free congelation ice (Fig. 1), there is the potential and need to
27 detect and quantify methane bubbles with optical remote sensing. In this study, we explored
28 high-resolution optical remote sensing images to study methane ebullition at Goldstream
29 Lake, an interior Alaska thermokarst lake (Fig. 1). We first mapped ebullition bubbles trapped
30 in early winter lake ice in aerial images. We refer to the bubble features seen in our images as
31 ‘bubble patches’ henceforth since the image resolution was not sufficient to fully resolve
32 small individual bubbles (Fig. 1). Then we characterized imaged bubble patches based on
33 field-based ebullition bubble seep data collected approximately 1-2 weeks after image




 Nombre : 1 Auteur : Sujet : Commentaire sur le texte Date : 2015-10-28 14:38:30


why is gas dissolved in water affecting ice backscattering properties caused by bubbles trapped in ice? Is this only affecting the properties of the bottom of ice cover (late winter), but that can also be seen with SAR?

 Nombre : 2 Auteur : Sujet : Commentaire sur le texte Date : 2015-10-28 14:38:44

why starting the sentence with "in contrast" then?

 Nombre : 3 Auteur : Sujet : Commentaire sur le texte Date : 2015-10-28 14:39:13

is this necessary?

 Nombre : 4 Auteur : Date : 2015-10-28 14:41:11

I suggest to make sure all these considerations are important to the introduction because it is a little long now.

1 acquisition in the fall of 2011 and 2012 and again in spring of the following year. We
2 hypothesized that the brightness of bubble patches correlates with the strength of methane
3 flux associated with four classes of ebullition bubble seeps (A, B, C and Hotspot) identified
4 by Walter Anthony et al. (2010). We estimated from aerial photos the bubble patch density
5 for each seep class as well as the mean whole-lake seep ebullition, examined the spatial
6 patterns of seep locations in the lake with respect to eroding thermokarst shores, and analyzed
7 spatio-temporal variability of seep occurrences by comparing imagery from different years.

8

9 **2 Study Site**

10 Goldstream L. is an interior Alaska thermokarst lake covering an area of approximately
11 10,300 m² with maximum and average depths of 2.9 m and 1.6 m, respectively. The lake
12 formed in ‘yedoma-type’ deposits of retransported late-Quaternary loess at the toe slope of
13 Goldstream Valley near Fairbanks (Péwé, 1975; Kanevskiy et al., 2011; Walter Anthony and
14 Anthony, 2013). Based on remotely-sensed aerial and satellite images, the lake partially
15 drained between years 1949 and 1978 but has been expanding mainly along the eastern shore
16 since then (Fig. 1f). This active thermokarst expansion is also indicated by spruce trees
17 leaning lake-ward along the eastern lake margin, and standing dead trees submerged in the
18 lake offshore of the eastern margin. The vegetation around the lake is dominated by black
19 spruce and willow. Cattail (*Typha* spp.) grows along some shallow margins of the lake. Water
20 lilies (*Nuphar* spp.) are also found in several locations on the northern and south-western parts
21 of the lake.

22 Ice formation on Goldstream L. usually occurs between the end of September to mid-October,
23 reaches maximum thickness by mid-March, and ice break up occurs around the end of April
24 or early May. Vertically oriented layers of methane ebullition bubbles (Fig. 1), representing
25 point-source seeps, are widespread in the lake ice particularly along the eastern margin
26 (Walter Anthony and Anthony, 2013). Many Hotspot seeps are also found near the eastern
27 eroding shore and are seen as open holes in lake ice during early winter and spring.

28

Cette page ne contient aucun commentaire.

1 **3 Methods**

2 **3.1 Ground truth field data**

3 We surveyed methane ebullition seep distribution on Goldstream L. using a survey-grade
4 LEICA VIVA™ real time kinematic Differential Global Positioning System (DGPS) with
5 centimeter-accuracy in fall 2011 and 2012 as well as spring 2012 and 2013. We surveyed the
6 lake perimeter and measured several permanently installed reference markers as Ground
7 Control Points (GCPs) to perform geometric rectification of aerial images. We conducted
8 detailed ebullition ice-bubble surveys in October 2011 two weeks after image acquisition. The
9 surveys were performed within two large polygons that are identified in Fig. 1f: One about ~
10 7 m from the eastern thermokarst shore and a second near the center of the lake. The surveyed
11 polygons in the east and center of the lake covered ~ 428 m² and ~ 236 m², respectively, and
12 were reported in detail in Walter Anthony and Anthony (2013) and Greene et al. (2014). In
13 October 2012, we performed bubble surveys 6 days after image acquisition in three other
14 polygons (total area ~ 200 m²) randomly distributed across the lake (Fig. 1f). We used the
15 seep identification method described by Walter Anthony et al. (2010), and included a fifth
16 class of ebullition seeps which we have observed in Goldstream L. and numerous other pan-
17 arctic lakes, called 'Tiny-type'. Tiny-type seeps consist of ebullition bubbles (typically 3 to 10
18 mm diameter) that form large (several to tens of square meters), diffuse patches rather than
19 clustering as tightly packed bubbles the way A, B, C and Hotspot seeps do. Until recently,
20 the Tiny-type seep class was only recorded in transect survey data but never assigned a mean
21 daily flux value or included in whole-lake ebullition estimates due to a lack of associated flux
22 data. Recent flux measurements made continuously year-round with submerged bubble traps
23 on the Tiny-type seep class in Goldstream. L. and other lakes suggest that flux from these
24 seeps may also be important (Walter Anthony et al., unpublished). Analysis of bubbles
25 collected with bubble traps placed over tiny-type seeps revealed that these bubbles were 60-
26 80% methane by volume. Here we report on the spatial extent of Tiny-type seeps as observed
27 in aerial imagery for Goldstream L., but we do not estimate their contribution toward whole-
28 lake ebullition flux.

29 While field-based estimations of A, B, and C-type seeps were limited to survey plots covering
30 about 13 % of the lake are, the locations of Hotspot seeps were mapped across the whole lake
31 using detailed DGPS surveys of open holes in October and April 2011 and 2012. Hotspots
32 were detected visually at these times of year as open-water holes in lake ice. In April 2013,

Cette page ne contient aucun commentaire.

1 we extracted several blocks of the full lake-ice column at seep locations to investigate the
2 temporal ebullition patterns that developed throughout the winter season.

3 **3.2 Remotely sensed high-resolution image acquisition**

4 We scheduled low altitude, high-resolution aerial image acquisitions to map and characterize
5 methane ebullition bubbles during a narrow time window in the early winter, when first ice
6 had formed but was still snow-free. Images were acquired in nadir with a Navion L17a plane
7 using a Nikon D300 camera system mounted in a bellyport on 14 October 2011 and 13
8 October 2012, two and four days following freeze-up, respectively. Flight altitude for the
9 acquisitions was ~750 m asl in 2011 and ~587 m asl in 2012. Image scale was 1:20,000 and
10 1:17,000 respectively for 2011 and 2012, which in turn corresponds to ground sampling
11 distance (GSD) of 11 cm and 9 cm. Additionally, we collected images of the snow-covered
12 lake in fall 14 October 2012 using an Unmanned Aerial Vehicle (UAV) mounted with an
13 Aptina MT9P031 board camera to map ice-free Hotspot seep locations. The images were
14 acquired from a flying height of approximately 230 m asl, corresponding to an image scale
15 1:30,000 and GSD of 6 cm. All the images consisted of three visible bands: red, green and
16 blue (RGB).

17 **3.3 Mapping bubble patches in early winter snow-free lake ice images**

18 We initially performed mosaicking of multiple images of Goldstream L. to construct a
19 complete image of the lake. This was achieved by using Agisoft PhotoScan Professional
20 Software™ Version 0.9.0. We then performed geometric image rectification with DGPS-
21 collected GCPs using a second polynomial bilinear transformation. Finally, for image
22 enhancement we applied a feature linear transformation on all three visible spectral bands of
23 the lake images using unstandardized Principal Component Analysis (PCA). Both geometric
24 and spectral image transformations were performed in ENVI™ image processing software,
25 Version 4.8.

26 Multi-spectral remote sensing data consists of high inter-band correlation and therefore bands
27 within a dataset carry redundant information (Rocchini et al., 2007). PCA transforms a set of
28 correlated variables (original bands) into a set of linearly uncorrelated orthogonal components
29 (principal components) (Schowengerdt, 2007; Estronell et al., 2013). It reduces the
30 dimensionality of the data and outputs the maximum amount of information with a physical

Cette page ne contient aucun commentaire.

1 meaning from the original bands into the least number of principal components (Estronell et
2 al., 2013). After transformation, the first principal component has the variables that account
3 for the most variance in the dataset and each succeeding independent component in turn
4 carries less and less of the original data variance. In our case, the first PC band (PC 1) carried
5 the most variance (> 98%) attributing to bubble patches (Fig. 2). Visually, bubble patches on
6 the lake ice appeared as dark patches in PC 1 band with low PC 1 grey values and were quite
7 distinct from the surrounding lake ice.

8 We then applied a classification technique based on object-based image analysis (OBIA) to
9 semi-automatically identify and map methane ebullition bubble patches in the PCA-
10 transformed images using eCognition Developer™ 8 (Lindgren et al. in prep). Our object-
11 based classification method comprised of two steps: (1) image segmentation, i.e. aggregation
12 of homogenous image pixels based on their spatial and spectral homogeneity into meaningful
13 clusters known as image objects, and (2) classification of image objects (Navulur, 2007;
14 Blaschke and Strobl, 2001). Varying ice conditions on the lake such as (a) clear, dark
15 congelation ice, (b) milky white snow-ice, and (c) ice with shadows from neighboring trees
16 added challenges to identifying ebullition bubble patches. We were able to resolve these
17 challenges by integrating semantic information associated with image objects in
18 classification. For this, we first decomposed our scene into meaningful regions. We then
19 organized them in a conceptual image object hierarchy creating a semantic network between
20 different sized image objects; large-scale objects in the upper level called super objects and
21 small-scale objects in the lower level called sub-objects (Supplement Fig. SI). For example,
22 the lake area is a super-object of different sub-objects associated with various lake ice
23 characteristics (e.g. shadow, dark black ice) whereas areas of specific lake ice characteristics
24 are super-objects of our final target feature, ebullition bubble patches. In each object level,
25 image objects within the boundary of super-objects were altered and refined through merging
26 and segmentation to form sub-objects with 1:n relationship between super- and sub-object. At
27 an early stage, we applied coarser image segmentation (i.e. broad scale segmentation) and
28 classification to delineate and label coarser target regions. Then in the later stages, finer
29 segmentation (i.e. fine scale segmentation) and classification was performed to delineate and
30 label finer target regions. This approach of detecting image objects from coarser to finer scale
31 has been described as an effective way to classify images in OBIA (Blaschke et al., 2008).

Cette page ne contient aucun commentaire.

1 Based on empirical performance tests, we used the first two PCA components (PC 1 and PC
2 2) to perform multi-resolution segmentation embedded in eCognition Developer™ software
3 to create image objects (eCognition Developer 7 Reference, 2007a). The advantage of using
4 multi-resolution segmentation is that it allows to create objects of different scales while
5 minimizing the heterogeneity within the resulting object at the given scale (Batz and Schape,
6 2000). For example, we applied a large-scale factor to create objects of different lake ice
7 characteristics and a small-scale factor to create bubble patch objects. We treated regions such
8 as areas of lake ice characteristics independently to perform region-specific classification for
9 the identification of target features within the domain of that particular region. In general, for
10 classification we used spectral characteristics in PC bands 1 and 2, contextual information
11 pertaining to image objects such as an image object's relationship with its neighbors and sub-
12 and super-objects, a Canny edge detection algorithm (Canny, 1986; eCognition Developer 7
13 Reference, 2007b) and morphological filters available in the eCognition Developer™
14 software.

15 The classification method performed very well in identifying bubble patches (Fig. 2) with an
16 overall accuracy of 98% when compared to manually identified bubble features in image
17 segments that served as our ground truth sample data for classification accuracy assessment.

18 Similarly, Hotspots that appeared dark against the snow-covered lake were mapped using a
19 simple contrast and split segmentation technique in eCognition Developer™ (eCognition
20 Developer 7 Reference, 2007a). This involved choosing a threshold value for the algorithm to
21 maximize the contrast between Hotspots and snow-covered lake pixels and separate them into
22 dark objects (consisting of pixels below the threshold) and bright objects (consisting of pixels
23 above the threshold).

24 **3.4 Interpretation of image classification results**

25 We extracted PC 1 grey values of individual ebullition bubble patches mapped in images from
26 the year 2011 and 2012. Bubbles patches are visually bright in natural or true color composite
27 (RGB composite) images but have low grey values in the PC 1 band (Fig. 2). A higher
28 brightness of bubble patches in natural color images resulted in lower PC 1 grey values. We
29 assessed the relationship of ebullition bubble patch PC 1 values with four distinct types of
30 ebullition seeps that we identified during our field survey. We performed an analysis of
31 variance (ANOVA) to test the null hypothesis that the mean PC 1 values (and thus true bubble

Cette page ne contient aucun commentaire.

1 brightness via its inverse relationship with the PC 1) of four types of seeps are not
2 significantly different. We proposed to apply a post-hoc Tukey's Honestly Significant Test
3 (HSD), if the null hypothesis was rejected, to identify significantly distinct seeps. We applied
4 a supervised classification using a Maximum Likelihood Classifier (MLC) on the three
5 original visible bands and their PC 1 component to classify mapped bubble patches into four
6 distinct seep classes. The MLC estimates a Bayesian Probability Function from the input
7 training classes and each pixel in the image is then assigned to the class with the highest
8 probability (Mather, 2009). Training samples were collected randomly on the image at seep
9 locations identified using field-collected DGPS data points. Since MLC was solely performed
10 on spectral characteristics derived from the training samples, the classification results from
11 MLC were further investigated to check the classification type and size of the seep mapped
12 within a bubble patch. Based on bubble morphology described by Walter Anthony et al.
13 (2010) and our field observations, we further refined our classification results by integrating
14 size as an additional feature to more accurately assign bubble patches with a seep type.
15 Similar to training sample collection, for accuracy assessment, field-collected seep location
16 data served as our ground truth. Finally, we estimated the seep density and mean whole-lake
17 ebullition rate by assigning the mean long-term flux values for seep type provided by Walter
18 Anthony and Anthony (2013) to our classified bubble patches.

19 We further studied the spatial distribution of ebullition bubble patches as a function of
20 distance from the eroding eastern thermokarst shore. For this, we divided the lake area into
21 multiple 5 m wide zones starting from the eastern eroding margin as mapped in a 1949 aerial
22 image. Lake zones were created on both sides of the 1949 lake margin to cover the present
23 day lake area. We calculated the percent of lake ice area covered with ebullition bubble
24 patches for each zone and then analyzed its relationship to the distance from the eastern shore
25 lines of the lake observed in 1949, 1978 and 2012.

26 We finally evaluated the multi-temporal (year 2011 and 2012) variability of ebullition bubble
27 patches and assessed their regularities in space and time. We utilized a marked point process
28 model to analyze spatial seep patterns in our multi-year bubble patch dataset derived from the
29 images. Point process modeling was performed on a set of bubble patch centroids with their
30 respective location and year information, which served as marked point dataset for the model,
31 to derive and test the spatial characteristics of bubble patch distribution against a null
32 hypothesis based on Complete Spatial Randomness (CSR). CSR suggests that the events are

Cette page ne contient aucun commentaire.

1 created by a random process over the study area and thus are independent from each other
2 (Bivand et al., 2008). For this, we generated a Multi-type Nearest Neighbor Distance Function
3 derived from the locations of the bubbles mapped in the images using *Gcross* from the
4 spatstat statistical package in R (Baddeley and Turner, 2005). *Gcross* first determines
5 clustering parameters for the dataset in the first year. These clustering parameters are then
6 used to model the expected number of the second year point given a certain distance from the
7 first year points if the second year point placement is random relative the first year point
8 placement. Thus, the *Gcross* function allowed us to describe seep clustering on the lake and
9 compare that with the theoretical value generated based on the assumption that seep locations
10 are completely random. Based on the deviation between observed empirical value and
11 expected theoretical value estimated by the model, we determined the stability of seep
12 locations between 2011 and 2012. Similarly, we performed the Multi-type Nearest Neighbor
13 Distance Function analysis using *Gcross* on the field dataset of Hotspot locations collected in
14 year 2011 and 2012 to check regularity of Hotspots.

15 We also considered that the centroid of a bubble patch, representing an ebullition bubble
16 patch point location, could move from one year to another due to changes in the shape and
17 size of a bubble patch or changes in bubble tube configuration in the sediment. We compared
18 the overlap area between ebullition patches mapped in 2011 and 2012 images. If some area of
19 a 2011 bubble patch appeared within the area of a 2012 bubble patch or vice versa, then we
20 considered bubble patch to be stable in location (i.e. reappearing). We assumed that the
21 overlapping bubble patches originated from the same point source seep. We checked location
22 stability among four classes of overlapping patches that were defined by setting thresholds on
23 area overlap; ‘All overlapping bubble patches’, ‘More than 25% area overlap’, ‘More than
24 50% area overlap’, ‘More than 75% area overlap’.

25 We used a map of ice-free Hotspots seeps derived from UAV images to compare the
26 frequency of Hotspots with Hotspot occurrences observed during multiple years of fieldwork
27 by Greene et al. 2014.

28

Cette page ne contient aucun commentaire.

1 **4 Results and discussion**

2 **4.1 Characteristics of bubble patches in early winter lake ice imagery**

3 **4.1.1 Relationship between bubble patch brightness and field-measured** 4 **methane flux**

5 We found that PC 1 values of bubble patches negatively correlated with the strength of field-
6 measured methane flux of ebullition seeps (A, B, C and Hotspot seeps). Our ANOVA test
7 rejected the null hypothesis suggesting significant distinction between mean PC 1 grey values
8 of different seep types. Further post-hoc analysis using Tukey's HSD test demonstrated that
9 C- and A-type, Hotspot and A-type, Hotspot and B-type seeps are significantly distinct with
10 p-values < 0.05 based on their mean PC 1 at a 95% confidence interval (Supplement Table
11 SI). We thus conclude that higher flux seeps, Hotspot and C-type, are associated with brighter
12 bubble patches (low PC 1 values) and lower flux seep types A and B are associated with less
13 bright bubble patches (high PC 1 values).

14 An absolute discrimination of individual seep type was difficult to achieve due to overlapping
15 brightness ranges between different seep types (Fig. 3). This is likely because ebullition is
16 episodic with varying bubbling rates over time and because individual low-flux methane
17 seeps were not resolved given spatial resolution of the image. A possible explanation for low
18 true brightness (high PC 1 values) of some Hotspots is that fresh thin night-time ice
19 temporarily covered some Hotspots on the image acquisition day, allowing the formation of
20 few small white gas bubbles while much of the remaining gas escaped through cracks in the
21 thin ice, resulting in low true brightness for these high-flux seeps. We have observed this
22 phenomenon on several occasions during our field visits in early winter and spring
23 particularly on days when temperatures stayed low and Hotspots were covered with a few
24 millimeters of ice with small bubbles beneath (Fig. 4); these Hotspots usually open up when
25 atmospheric temperature rises again during the day. Conversely, Hotspots that remained ice-
26 free could not be identified in our snow-free lake ice imagery due to spectral similarities
27 between open water and clear black ice (Fig. 1).

28 We found that a large number of A-type seeps clustered together were not mapped as
29 individual bubble patches but rather as a single large bubble patch. A-type seeps and high flux
30 seeps that were close together were also mapped in a single feature associated with a brighter
31 bubble patch with low PC 1 values. Therefore, some A-type seeps showed low PC 1 values

Cette page ne contient aucun commentaire.

1 (high true brightness). Similar to A-type seeps, individual B-type seeps were also difficult to
2 map. In a time series analysis of bubbling frequency by A- and B-type seeps, Walter Anthony
3 et al. (2010) showed that bubbling from these shallow-sourced seeps is highly seasonal.
4 Bubbling rates are high in summer when surface sediments are warmer, and low in winter
5 when sediments cool down. Bubble traps left in place over these seep types year-round
6 revealed that low-flux seeps can have periods of no bubbling for up to several months. Ice
7 blocks harvested by us in spring over seeps marked as A-type seeps in October confirm this
8 pattern (Supplement Fig. SII). It is very likely that A- and B-type seep conduits were present
9 in the sediments, but not actively bubbling during the two- and four-day periods after ice
10 formation captured by the 2011 and 2012 imagery. Thus they did not appear under the given
11 spatial resolution of the image and its specific acquisition time. Also, bubble traps placed over
12 C-type seeps year round revealed that these seeps can also undergo long periods (weeks to
13 months) of no bubbling, but when they bubble, the bubbling rates are usually very high
14 (Walter Anthony et al., 2010). This intermittent flux behavior probably contributed to some
15 discrepancies in the relationship between bubble patch brightness derived from images that
16 captured a snapshot of ebullition activity and methane flux values of seeps estimated from
17 long-term field observations (Table 1).

18 In other parts of Goldstream L., especially along the eastern shore, we found large patches of
19 Tiny-type seeps. When we extracted an ice block in spring 2013, we observed that Tiny-type
20 ebullition had been frequent throughout winter, resulting in long, vertically oriented stacks of
21 tiny ebullition bubbles trapped in ice (Fig. 4). In our optical images, tiny-type ebullition
22 appeared as irregular patches of fuzzy, white-colored bright ice with some bright regular
23 bubble spots (Fig. 4). Therefore, the brightness values corresponding to the surrounding Tiny-
24 type seeps were assigned to other seeps, particularly to low flux seeps that were within the
25 Tiny-seep patch and had not expressed completely when the images were acquired.

26 **4.1.2 Classification of bubble patches and estimation of whole-lake methane** 27 **flux**

28 The overall MLC classification accuracy for differentiating seep types was ~ 50% for both
29 2011 and 2012 with better performance in the 2012 image with 55% accuracy. The classifier
30 performed better to identify the lowest flux seeps (A-type) and the highest flux seeps
31 (Hotspot-type). B-type and C-type seeps showed high error of commission mostly rising from

Cette page ne contient aucun commentaire.

1 the misidentification of seep A-type and Hotspots. C-type seeps had the largest error of
2 omission since they were mostly misclassified as B-type seeps in 2011 and Hotspots in 2012.

3 Generally higher densities of A-type seeps (and also slightly in B- and C-type seeps) in
4 ground surveys (Walter Anthony and Anthony, 2013; Greene et al., 2014) compared to aerial
5 images (Table 1) can be explained by the time in which observations were made and image
6 resolution. Results reported in Walter Anthony and Anthony (2013) and Greene et al. (2014)
7 are based on ground surveys conducted at Goldstream L. usually one to two weeks following
8 freeze-up when ice was safe to walk on (Walter Anthony et al., 2010). Since our aerial
9 surveys were conducted only 2-4 days after ice formation, and the frequency of bubbling
10 events from A-type seeps is often weeks to months in winter, it is not surprising that the field
11 surveys several weeks after ice formation capture an order of magnitude more A-type seep
12 bubbles. Additionally, it is very likely that some active A-type seeps that occurred in very
13 small patches were not distinct under the given resolution of the aerial images. Relatively
14 more frequent bubbling in B- and C-type seeps allows for similar seep density values between
15 ground surveys and aerial images; however, as expected, the 2012 seep densities are closer to
16 the ground-ice survey values due to (a) more time since freeze-up and (b) a much higher
17 barometric pressure drop preceding the aerial image acquisition in October 2012 compared to
18 October 2011. It is well established that ebullition is inversely related to changes in
19 barometric pressure (Mattson and Likens, 1990; Fechner-Levy and Hemond, 1996; Scandella
20 et al., 2011).

21 The comparison of Hotspot densities in optical images vs. ground surveys in Table 1 also
22 shows the expected pattern. The ground-survey data of Hotspots reflects multiple years of
23 whole-lake Hotspots surveys when ice is thick enough to safely walk on. When ice is very
24 thin a few days after freeze up more open holes are present on the lake and classified as
25 Hotspot seeps in aerial images. A week or more later many holes freeze over and will be
26 classified as C-type seeps in ground surveys. This could have also led to a high classification
27 error for C-type seeps. The total density of C-type and Hotspot seeps combined remain
28 consistent (~ 0.04 seeps m^{-2}) in both aerial and ground observations (Table 1). This also
29 indicates that some of the seeps identified as Hotspots several days after freeze-up in aerial
30 photos really become what we classify as C-type seeps (ice-sealed at the surface) within a
31 week or more following freeze up.


Cette page ne contient aucun commentaire.


1 We used the classification results to estimate seep density and a whole-lake ebullition rate.
2 Our image-based analysis shows the whole-lake flux to be 174 ± 28 ml gas $m^{-2} d^{-1}$ and $216 \pm$
3 33 ml gas $m^{-2} d^{-1}$ for the year 2011 and 2012, respectively. The higher flux estimate in 2012
4 is due to the presence of a ¹large number of bubble patches in 2012 (0.185 seeps m^{-2})
5 compared to 2011 (0.119 seeps m^{-2}) (Table 1). ²The field-based estimate of whole-lake
6 ebullition for Goldstream L. using ice-bubble transect surveys (170 ± 54 ml gas $m^{-2} d^{-1}$), was
7 slightly at the low end of the estimates based on optical imagery analysis from 2011 and 2012
8 respectively. It is conceivable that the field-based transect surveys might yield a lower flux
9 than whole-lake seep analyses given that seeps are spatially rare, and field surveys often cover
10 $<1\%$ of the lake surface area (Walter Anthony and Anthony, 2013). However, on Goldstream
11 L., where our field transect bubble surveys covered 13% of the lake area for A, B and C-type
12 seeps and 100% of the lake area for Hotspots, ³the higher estimates based on optical imagery
13 appear to be due to an overestimation of Hotspots in the early-acquisition date aerial image
14 analysis.


15 **4.2 Spatial and temporal characteristics of bubble patches on early winter** 16 **lake ice**

17 **4.2.1 Spatial distribution of bubble patches in relation to thermokarst-lake** 18 **margin**

19 High methane production in response to thermokarst activity on the Goldstream L. is also
20 evident from the distribution pattern of ebullition bubble patches at the eroding margins in
21 different years. We found a strong inverse relationship (R^2 values of 0.86 and 0.79 for the
22 years 2011 and 2012, respectively) between ebullition bubble patch area covering the lake ice
23 and distance from the rapidly eroding eastern margin of the lake (Fig. 5). The percent surface
24 area of lake ice covered with ebullition bubble patches ice decreased with distance from the
25 active erosion margin. Thermo-erosion as well as talik growth on the expanding eastern shore
26 release labile Pleistocene-aged organic matter as permafrost thaws, enhancing anaerobic
27 microbial activity in the lake and talik sediments, and leading to enhanced methane emissions
28 along this shore (Brosius et al., 2012; Walter Anthony and Anthony, 2013). Holocene-aged
29 carbon from vegetation and active layer soils is also eroded and additionally produced within
30 the lake, further fueling microbial methane production (Walter Anthony et al., 2014). We
31 observed fewer ebullition bubble patches in the center of the lake, which we interpret as a

 Nombre : 1 Auteur : Sujet : Commentaire sur le texte Date : 2015-10-28 13:47:37
larger?

 Nombre : 2 Auteur : Sujet : Commentaire sur le texte Date : 2015-10-28 14:41:26
done on what year? both?

 Nombre : 3 Auteur : Sujet : Commentaire sur le texte Date : 2015-10-28 13:49:53
higher only in 2012

1 sign that labile Pleistocene-aged organic carbon in the talik under this area has been largely
2 depleted, and unlike at the edge along the active erosion margin, there is no significant
3 additional accumulation of ancient labile carbon in the lake center (Brosius et al., 2012).
4 Radiocarbon dating of bubble patches found in the lake center showed that these seeps
5 originate from Holocene-aged and more recent organic matter that is found in the upper lake
6 sediments (Brosius et al., 2012). Generally, methane bubbling was the lowest along the 1949
7 eastern lake margin and the highest along the 2012 eastern lake margin (Fig. 5), indicating
8 that depletion of labile carbon progressed since these areas were included in the lake and the
9 active thermo-erosion margin migrated eastward. This shows that optical remote sensing is a
10 powerful tool to understand the spatial variability of methane ebullition on thermokarst lakes.

11 **4.2.2 Multi-year comparison of bubble patch characteristics: 2011 and 2012**

12 We observed four possible characteristics of bubble patch dynamics in our images (Fig. 6). (a)
13 Bubble patches may move horizontally; (b) Bubble patches **don't** maintain the same
14 morphology between years (e.g. single bubble patches re-appear in a cluster of multiple
15 patches the next year or vice-versa); (c) Bubble patches appear in an image in one year and
16 not another; and (d) Bubble patches maintain the location and shape but patch size is different
17 between the years. It is important to note that these observations are made during the two very
18 short windows of time 2-4 days after freeze-up. Our analysis does not take into account the
19 changes in long-term bubble patch morphology. Hence, it is important to highlight that the
20 characteristics of bubble patches are driven by the dynamics of bubble formation and
21 transport, hydrostatic pressure, and ice growth. Other changes in the characteristics of bubble
22 patches could be because of evolution of point sources or changes in point source conduits
23 (bubble tubes) in the sediment (Walter et al., 2008a; Scandella et al., 2011). Atmospheric
24 pressure dynamics can also strongly impact bubbling over short time scales, resulting in
25 different ice-bubble patterns one year from the next if insufficient time passes to allow all
26 seeps to be expressed in the lake ice cover. Field measurements have shown that ebullition is
27 inversely related to changes in hydrostatic pressure (Mattson and Likens, 1990; Varadharajan,
28 2009; Casper et al., 2000; Glaser et al., 2004; Tokida et al., 2007; Scandella et al., 2011). A
29 significant air pressure drop during the week preceding image acquisition in October 2012
30 may have allowed methane that previously accumulated in the sediment during high-pressure
31 days to rise up into the water column, manifesting itself as larger numbers of bubbles and
32 larger bubble-patch sizes in the lake ice (Fig. 7). Conversely, air pressure change in October

1 2011 was not large enough to enhance ebullition before the image was acquired. As a result,
2 bubble patch density was 55% higher in 2012 (0.185 m^{-2}) ~~2012~~ compared to 2011 (0.119 m^{-2}).
3 Similarly, the estimated mean whole-lake ebullition was 24% higher in 2012 compared to
4 2011. However, the general spatial distribution of bubble patches remained the same between
5 the two years: ebullition bubble patches were more concentrated towards the eastern
6 thermokarst lake shore.

7 The *Gcross* distribution functions for marked bubble patch locations derived from images and
8 for Hotspot locations derived from DGPS field datasets agree on regularities of seep locations
9 across time (Fig. 8). The deviation between the observed empirical value (black curve) and
10 theoretical expected value assuming the points are completely random (red curve) in *Gcross*
11 function, suggests that a large and statistically significant number of bubble patches and
12 Hotspot seeps show spatial dependence between years 2011 and 2012 (Fig. 8). The empirical
13 curves in both cases lie well above the gray shaded area, which is the 95% critical confidence
14 band for theoretical assumption of complete spatial randomness and independence. The plot
15 for bubble patch distribution function shows that a statistically significant number of second
16 year bubble patch center points are less than 2 meters away from the first year center points.
17 The observed function for the DGPS Hotspot locations rises almost vertically over separation
18 distances of 0-1 meter deviating away from the theoretical function. Therefore, we conclude
19 that the seep locations are consistent between years 2011 and 2012. Based on our DGPS data,
20 the number of Hotspots was relatively stable among the various surveys with about 105
21 Hotspots for the whole lake as the average of various measurements during different years
22 and spring and fall field seasons (Greene et al., 2014). UAV-based aerial images taken five
23 days after ice formation when snow covered the lake also demonstrated close agreement with
24 the Hotspot seep numbers and locations. We were able to identify 78 dark open-water holes in
25 the white, snow-covered UAV lake image acquired in early winter of 2012. Among these 78
26 locations there was a total of about ~ 95-100 active ice-free Hotspot seeps since some large,
27 irregularly shaped holes consisted of multiple, coalesced holes produced by Hotspot seeps of
28 close proximity (Supplement Fig. SIII).

29 When we compared the location of bubble patches in 2011 and 2012, we found that 47.2% of
30 total 1195 ebullition bubble patches mapped in 2011 reappeared in 2012, which is 35.7% of
31 total 1860 ebullition bubble patches mapped in 2012 (Table 2). Using thresholds of area
32 overlap in our evaluation of seep location stability we found that 37.5%, 30% and 17.7% of

1 bubble patches mapped in 2011 reappeared when we considered bubble patches with ‘more
2 than 25% area overlap’, ‘more than 50% overlap’ and ‘more than 75% area overlap’,
3 respectively. We expect that if more time passed between the time of freeze-up and aerial
4 image acquisition date we would see an even higher percentage of seep location re-
5 occurrences because more seeps would be actively expressed.

6 We also observed a relationship between bubble patch brightness and location stability of
7 bubble patches. Very bright patches in 2012 seemed to appear at locations where bubble
8 patches were already observed in 2011. Increased brightness in 2012 of re-occurring
9 ebullition bubble patches could indicate locations of high flux seeps where methane was able
10 to rise through the sediment even in relatively high hydrostatic pressure conditions that we
11 observed in October 2011. Based on our bubble patch classification results (Table 1), we also
12 noticed that seep density of high-flux C- and Hotspot-type seeps is less variable during our
13 study period compared to low-flux A- and B-type seeps. However, long-term remote sensing
14 and ground-based observations are required to further test our hypothesis.

15 The regularity of bubble patches observed despite the differences in atmospheric pressure
16 conditions following the lake freeze-up events in 2011 and 2012 as well as the location
17 stability of Hotspots indicates that a large number of point source seeps in thermokarst lakes
18 are stable over at least annual time-scales. Walter Anthony et al. (2010) also found seeps to
19 maintain stable locations in Goldstream L. when submerged bubble traps were placed over
20 individual seeps to monitor their ebullition dynamics for periods of up to 700 days. In Siberia
21 one Hotspot seep location was marked and found stable for at least eight years (Walter
22 Anthony et al., 2010).

23

24 **5 Benefits and challenges of aerial image analysis for ebullition seep** 25 **mapping**

26 Our results show that ebullition bubble patches can be mapped to high precision in aerial
27 imagery. But because ebullition is a temporally dynamic phenomenon, our ability to
28 accurately identify the distinct seep type of bubble patches on a snapshot of ebullition activity
29 during only 2- and 4-days since lake ice formation is limited. The morphology and
30 distribution of bubbles can undergo significant changes in response to freeze/thaw cycles
31 during winter (Jeffries et al., 2005). Furthermore, ebullition is highly controlled by the
32 balance between atmospheric pressure and sediment strength making it an episodic

Cette page ne contient aucun commentaire.

1 phenomenon (Varadharajan, 2009; Scandella et al., 2011). Ebullition is triggered following
2 the falling of hydrostatic pressure or after a sufficient volume of gas is produced in the
3 sediment that allows “bubble-tubes” or “gas conduits” in lake sediments to open or dilate
4 (Scandella et al., 2011). Bubbles previously trapped in lake sediment then break out through
5 these open “bubble-tubes” and rise up in the water column. Moreover, microbial activity of
6 methane producing bacteria is temperature dependent. As a result, seep ebullition slows down
7 when the lake surface sediments cool down in winter and it increases as lake sediment warms
8 up in summer (Walter Anthony and Anthony, 2010). Therefore, discrepancies arise in
9 estimates of the number of seeps and seep morphology derived from observations made at
10 different times of the ice cover season (Wik et al., 2011).

11 Ideally, optical image acquisition would occur at least several weeks following freeze-up of
12 lakes to allow more time for seep expression in lake ice. Unfortunately, snow-free conditions
13 several weeks after freeze-up is rare in many regions of the Arctic and early snow cover
14 inhibits the mapping of bubble patches with optical data. Despite these challenges, we found
15 numerous significant benefits of using aerial images for characterizing ebullition seeps on
16 lake ice. Aerial images of early winter lake ice without snow cover allow to map and
17 characterize bubble patches on the entire lake surface as well as assess their spatial
18 distribution more accurately. We were able to differentiate high methane emitting seeps from
19 low methane emitting seeps on the lake based on bubble patch brightness. Image-derived
20 estimates of seep densities by class agreed with those of field-based survey methods, except
21 for the understandable problems of overestimating Hostspots and underestimating A-type
22 seeps. We were able to differentiate lake areas with high seep densities versus low seep
23 densities; this ability could be especially important on larger lakes that are harder to survey
24 extensively by foot. Thus, our study shows that remote sensing methods have the potential to
25 be very helpful for improving understanding of ebullition spatial variability and microbial
26 processing of organic matter within an individual lake. ¹Our results also imply a potential to

27 apply high resolution optical images at a regional scale to quantify relative methane flux from
28 other lakes, which at a minimum should allow for classification of high-ebullition versus low-
29 ebullition lakes and their distribution in a region. It is important to note, that while image

30 analysis is useful to comprehensive mapping of lake-ice bubbles, for estimation of whole-lake
31 methane emissions, this technique should be coupled with field measurements of bubble
32 collection using bubble traps and laboratory measurements of methane concentration in
33 bubbles.

Nombre : 1 Auteur : Sujet : Commentaire sur le texte Date : 2015-10-28 14:42:15

It could be interesting that you mention if these images are expensive (or free)? One could wonder if this is affordable when 100km² is 2-3K (?) for pan-arctic estimations.

1 Finally, a lake's capacity to produce methane can tell us about the permafrost characteristics
2 in the lake area. For example, yedoma-type thermokarst lakes such as Goldstream L., where
3 large amount of labile carbon is readily available for microbes to decompose, emit more
4 methane than non-yedoma-type thermokarst lakes (Walter Anthony and Anthony, 2013;
5 Sepulveda-Jáuregui et al., 2014). This differentiation could be used for identifying presence
6 or absence of organic-rich permafrost deposits such as yedoma in the area and can be a useful
7 supplement to surveying soil carbon pools and yedoma distribution.

8

9 **6 Conclusions**

10 It is important to understand the dynamics of methane ebullition from thermokarst lakes to
11 estimate the amount of carbon release from thawing permafrost and evaluate its feedback to
12 the global carbon cycle. Our study focusing on Goldstream L., Interior Alaska, shows that
13 high-resolution optical remote sensing is a promising tool to map the distribution of point
14 source methane ebullition seeps across an entire thermokarst lake surface, a task that is
15 difficult to achieve through field-based surveys alone.

16 Statistical analysis of mapped bubble patches allowed differentiation between low-flux (A-
17 and B-type seeps) and high-flux (C-type seeps and Hotspots) methane ebullition seeps on the
18 lake. Multi-temporal analysis of bubble patches mapped in 2011 and 2012 images indicated
19 variability in ebullition seep densities on the lake. We observed more active ebullition (i.e. a
20 higher density of seeps) in 2012 coinciding with low atmospheric pressure preceding the
21 image acquisition while high-pressure condition suppressed ebullition activity in 2011. It is
22 possible that the twice as long period of ice formation and bubble accumulation in 2012 (4
23 days) compared to 2011 (2 days) also contributed to the observation of more seep activity in
24 the early days following freeze-up in 2012. Our mean whole-lake ebullition estimates for
25 2011 (174 ± 28 ml gas $m^{-2} d^{-1}$) and 2012 (216 ± 33 ml gas $m^{-2} d^{-1}$) using aerial image
26 analysis of the whole lake were slightly higher than the estimate based on field surveys of
27 only 13% of the lake conducted over multiple years (170 ± 54 ml gas $m^{-2} d^{-1}$). We found that
28 aerial image analysis of early-fall images tended to underestimate low-flux A-type seeps, but
29 overestimated the density of Hotspots, leading to total higher flux estimates than field-based
30 surveys. If more time were allotted between freeze-up and image acquisition (for instance the
31 1-3 weeks typically allowed for ground surveys), such that the infrequent bubbling of A's
32 could occur and a subset of open holes would freeze-over to be recognized as C-type seeps

Cette page ne contient aucun commentaire.

1 instead of hotspots, we expect that the densities of A- and Hotspot-type seeps as well as the
2 derived whole lake methane flux would be more similar between the aerial and the ground-
3 survey methods.

4 A large and statistically significant number of seeps were stable over our study period despite
5 the differences in atmospheric pressure and lake ice conditions only 2 and 4 days following
6 freeze-up. The general spatial distribution of seeps was very consistent in both years with a
7 strong inverse relationship between percent surface area of lake ice with bubble patches and
8 distance from an actively eroding thermokarst lake margin ($R^2 = 0.86$ and $R^2 = 0.79$ for 2011
9 and 2012 respectively). These findings indicate lake expansion by thermokarst activity to be
10 the dominating factor for high methane seep ebullition on Goldstream L.

11 Our study shows that remote sensing techniques can help overcome the shortcomings of a
12 sole field-based method of methane survey, particularly by revealing the location and relative
13 sizes of high- and low-flux seepage zones within lakes. However, the timing of image
14 acquisition is a critical and potentially limiting factor, with respect to both atmospheric
15 pressure changes and snow/no-snow conditions during early lake freeze up. Our approach is
16 applicable to other regions and will help to characterize methane ebullition emissions from
17 seasonally ice-covered lakes, including thermokarst and non-thermokarst lakes. Remotely
18 sensed, multi-temporal spatial information allows identification of variables that control
19 methane ebullition dynamics and spatial patterns to better estimate methane emission from
20 thermokarst lakes. Such observations may also be used to indirectly characterize permafrost
21 carbon storage since thermokarst lakes with greater numbers of high flux seeps adjacent to
22 margins of thermokarst expansion likely indicate the presence of organic-rich permafrost
23 deposits.

24 25 **Acknowledgements**

26 We thank A. Bondurant for harvesting ice blocks; P. Anthony for statistical coding; and A.
27 Strohm, M. Engram and J. Lenz for assistance with other field work. We thank J. Cherry for
28 aerial image acquisitions and B. Crevensten and G. Walker for UAV image acquisitions. This
29 research was funded by NASA Carbon Cycle Science grant #NNX11AH20G. Additional
30 support came from NSF # 1107892.

31

1 **Author contributions**

2 G. Grosse and K. M. Walter Anthony conceived this study. P. R. Lindgren developed the
3 method, performed data analysis, and wrote the manuscript with significant input from all co-
4 authors. P. R. Lindgren, G. Grosse and K. M. Walter Anthony were responsible for the field
5 work.

6

7 **References**

8 Baatz, M. and Schäpe, A.: Multiresolution segmentation - an optimization approach for high
9 quality multi-scale image segmentation. *Angewandte Geographische*
10 *Informationsverarbeitung XII, Beiträge zum AGIT-Symposium Salzburg 2000*, 12-23.
11 Herbert Wichmann Verlag, Karlsruhe, 2000.

12 Baddeley, A. and Turner, R.: Spatstat: An R package for analyzing spatial point patterns, *J.*
13 *Stat. Software*, 12(6), 1–42, URL: www.jstatsoft.org, ISSN: 1548–7660, 2005.

14 Bastviken, D.: Methane emissions from lakes: Dependence of lake characteristics, two
15 regional assessments, and a global estimate, *Global Biogeochem. Cycles*, 18(4), 1–12,
16 doi:10.1029/2004GB002238, 2004.

17 Bastviken, D., Tranvik, L. J., Downing, J. A., Crill, P. M., and Enrich-Prast, A.: Freshwater
18 methane emissions offset the continental carbon sink, *Science*, 331, 50, 2011.

19 Bivand, R. S., Pebesma, E. J., and Gomez-Rubio, V.: *Applied Spatial Data Analysis with R*,
20 Springer, New York, 2008.

21 Blaschke, T. and Strobl, J.: What’s wrong with pixels? Some recent developments interfacing
22 remote sensing and GIS, *GIS – Zeitschrift für Geoinformationssysteme*, 14 (6), 12–17, 2001.

23 Blaschke, T., Lang, S., and Hay, G. J.: *Object Based Image Analysis: Spatial Concepts for*
24 *Knowledge-Driven Remote Sensing Applications*, Springer-Verlag Berlin Heidelberg,
25 Germany, 2008.

26 Boereboom, T., Depoorter, M., Coppens, S., and Tison, J.-L.: Gas properties of winter lake
27 ice in Northern Sweden: implication for carbon gas release, *Biogeosciences*, 9(2), 827–838.
28 doi:10.5194/bg-9-827-2012, 2012.

Cette page ne contient aucun commentaire.

1 Brosius, L. S., Walter Anthony, K. M., Grosse, G., Chanton, J. P., Farquharson, L. M.,
2 Overduin, P. P., and Meyer, H.: Using the deuterium isotope composition of permafrost
3 meltwater to constrain thermokarst lake contributions to atmospheric CH₄ during the last
4 deglaciation, *J. Geophys. Res.*, 117(G1), G01022, doi:10.1029/2011JG001810, 2012.

5 Canny, J.: A computational approach to edge detection, *IEEE Trans. Pattern Analysis &*
6 *Machine Intelligence*, 8, 679-714, 1986.

7 Casper, P., Maberly, S. C., Hall, G. H., and Finlay, B. J.: Fluxes of methane and carbon
8 dioxide from a small productive lake to the atmosphere, *Biogeochemistry*, 49, 1–19, 2000.

9 Definiens, Segmentation Algorithms In Definiens Developer 7 Reference Book, Document
10 Version 7.0.0.843, 15-27, Definiens AG, München, Germany, 2007a.

11 Definiens, Edge Extraction Canny In Definiens Developer 7 Reference Book, Document
12 Version 7.0.0.843, 62-63, Definiens AG, München, Germany, 2007b.

13 Duguay, C. R. and Lafleur, P. M.: Determining depth and ice thickness of shallow sub-Arctic
14 lakes using space-borne optical and SAR data, *Int. J. Remote Sens.*, 24(3), 475–489,
15 doi:10.1080/01431160304992, 2003.

16 Engram, M., Walter Anthony, K. M., Meyer, F. J., and Grosse, G.: Characterization of L-band
17 synthetic aperture radar (SAR) backscatter from floating and grounded thermokarst lake ice in
18 Arctic Alaska, *Cryosph.*, 7(6), 1741–1752, doi:10.5194/tc-7-1741-2013, 2013.

19 Engram, M., Walter Anthony, K. M., Meyer, F. J., and Grosse, G.: Synthetic aperture radar
20 (SAR) backscatter response from methane ebullition bubbles trapped by thermokarst lake ice,
21 *Canadian Journal of Remote Sensing*, 38(6), 667–682, 2012.

22 Estornell, J., Marti-Gavila, J. M., Teresa Sebastia, M., and Mengua, J.: Principal component
23 analysis applied to remote sensing, *Modelling in Science Education and Learning*, 6(2), 83-
24 89, 2013.

25 Fechner-Levy, E. J. and Hemond, H. F.: Trapped methane volume and potential effects on
26 methane ebullition in a northern peatland, *Limnol. Oceanogr.*, 41(7), 1375–1383, 1996.

27 Glaser, P. H., Chanton, J. P., Morin, P., Rosenberry, D. O., Siegel, D. I., Ruud, O., Chasar, L.
28 I., and Reeve, A. S.: Surface deformations as indicators of deep ebullition fluxes in a large
29 northern peatland, *Global Biogeochem. Cycles*, 18, GB1003, doi:10.1029/2003GB002069,
30 2004.

Cette page ne contient aucun commentaire.

1 Greene, S., Walter Anthony, K. M., Archer, D., Sepulveda-Jauregui, A., and Martinez-Cruz,
2 K.: Modeling the impediment of methane ebullition bubbles by seasonal lake ice,
3 *Biogeoscience Discuss.*, 11, 10863–10916, 2014. <http://doi:10.5194/bgd-11-10863-2014>.

4 Grosse, G. et al.: Vulnerability of high-latitude soil organic carbon in North America to
5 disturbance, *J. Geophys. Res.*, 116, 1–23, doi:10.1029/2010JG001507, 2011.

6 Grosse, G., Jones, B., and Arp, C.: Thermokarst Lakes, Drainage and Drained Basins,
7 *Treatise Geomorphol.*, 8, 325–353, 2013.

8 Hinzman, L. D. et al.: Evidence and Implications of Recent Climate Change in Northern
9 Alaska and Other Arctic Regions, *Clim. Change*, 72(3), 251–298, doi:10.1007/s10584-005-
10 5352-2, 2005.

11 Hugelius, G. et al.: Improved estimates show large circumpolar stocks of permafrost carbon
12 while quantifying substantial uncertainty ranges and identifying remaining data gaps,
13 *Biogeosciences Discuss.*, 11(3), 4771–4822, doi:10.5194/bgd-11-4771-2014, 2014.

14 Jeffries, M. O., Morris, K., Weeks, W. F., and Wakabayashi, H.: Structural and stratigraphic
15 features and ERS 1 synthetic aperture radar backscatter characteristics of ice growing on
16 shallow lakes in NW Alaska, winter 1991-1992, *J. Geophys. Res.*, 99(C11), 22459–22471,
17 1994.

18 Jeffries, M. O., Morris, K., and Kozlenko, N.: Ice Characteristics and Remote Sensing of
19 Frozen Rivers and Lakes, *Remote Sensing in Northern Hydrology: Geophysical Monograph*
20 *Series*, 163, 63-90, 2005.

21 Jorgenson, M. T. and Shur, Y.: Evolution of lakes and basins in northern Alaska and
22 discussion of the thaw lake cycle, *J. Geophys. Res.*, 112(F2), 1–12,
23 doi:10.1029/2006JF000531, 2007.

24 Kanevskiy, M., Shur, Y., Fortier, D., Jorgenson, M. T., and Stephani, E.: Cryostratigraphy of
25 late Pleistocene syngenetic permafrost (yedoma) in northern Alaska, Ikillik River exposure,
26 *Quat. Res.*, 75(3), 584–596, doi:10.1016/j.yqres.2010.12.003, 2011.

27 Keller, M. and Stallard, R. F.: Methane emission by bubbling from Gatun Lake, Panama, *J.*
28 *Geophys. Res.*, 99, 8307–8319, doi:10.1029/92JD02170, 1994.

29 Kessler, M. A., Plug, L. J., and Walter Anthony, K. M.: Simulating the decadal- to millennial-
30 scale dynamics of morphology and sequestered carbon mobilization of two thermokarst lakes

Cette page ne contient aucun commentaire.

1 in NW Alaska, *J. Geophys. Res. Biogeosciences*, 117(G2), 1-22, doi:10.1029/2011JG001796,
2 2012.

3 Kokelj, S. V. and Jorgenson, M. T.: Advances in Thermokarst Research, *Permafr. Periglac.*
4 *Process.*, 24(2), 108–119, doi:10.1002/ppp.1779, 2013.

5 Koven, C. D., Ringeval, B., Friedlingstein, P., Ciais, P., Cadule, P., Khvorostyanov, D.,
6 Krinner, G., and Tarnocai, C.: Permafrost carbon-climate feedbacks accelerate global
7 warming, *Proc. Natl. Acad. Sci.*, 108, 14769–14774, doi:10.1073/pnas.1103910108, 2011.

8 Langer, M., Westermann, S., Walter Anthony, K. M., Wischnewski, K., and Boike, J.: Frozen
9 ponds: production and storage of methane during the Arctic winter in a lowland tundra
10 landscape in northern Siberia, Lena River Delta, *Biogeosciences Discuss.*, 11(7), 11061–
11 11094, doi:10.5194/bgd-11-11061-2014, 2014.

12 Mather, P.: *Pattern Recognition Principles In Classification for Remotely Sensed Data*,
13 *Second Edition*, 41-75, CRC Press, New York, 2009.

14 Mattson, M. D. and Likens, G. E.: Air pressure and methane fluxes, *Nature*, 347, 718–719,
15 1990.

16 Navulur, K.: *Multispectral Image Analysis Using the Object-Oriented Paradigm*, CRC Press,
17 Boca Raton, FL, 2007.

18 Péwé, T. L.: *Quaternary geology of Alaska*, U.S. Geol. Survey Professional Paper 835, 1975.

19 Phelps, A. R., Peterson, K. M., and Jeffries, M. O.: Methane efflux from high-latitude lakes
20 during spring ice melt. *J. Geophys. Res. Atmos.* 103:29029-29036, doi:10.1029/98JD00044,
21 1998.

22 Plug, L. J. and West, J. J.: Thaw lake expansion in a two-dimensional coupled model of heat
23 transfer, thaw subsidence, and mass movement, *J. Geophys. Res.*, 114(F1), F01002,
24 doi:10.1029/2006JF000740, 2009.

25 Rowland, J. C., Travis, B. J., and Wilson, C. J.: The role of advective heat transport in talik
26 development beneath lakes and ponds in discontinuous permafrost, *Geophys. Res. Lett.*,
27 38(17), 1–5, doi:10.1029/2011GL048497, 2011.

28 Rocchini, D., Ricotta, C., and Chiarucci, A.: Using satellite imagery to assess plant species
29 richness: The role of multispectral systems systems, *Applied Vegetation Science*, 10, 325-
30 332, 2007.

Cette page ne contient aucun commentaire.

1 Scandella, B. P., Varadharajan, C., Hemond, H. F., Ruppel, C., and Juanes, R.: A conduit
2 dilation model of methane venting from lake sediments, *Geophys. Res. Lett.*, 38(6), 1-6,
3 doi:10.1029/2011GL046768, 2011.

4 Schowengerdt, A.: *Principal Components In Remote sensing: Models and methods for image*
5 *processing*, Third Edition, 193-199, Academic Press, San Diego, CA, 2007.

6 Schuur, E. A. G. et al.: Vulnerability of Permafrost Carbon to Climate Change: Implications
7 for the Global Carbon Cycle, *Bioscience*, 58(8), 701, doi:10.1641/B580807, 2008.

8 Sepulveda-Jáuregui, A., Walter Anthony, K. M., Martinez-Cruz, K., Greene, S., and F.
9 Thalasso. Methane and carbon dioxide emissions from 40 lakes along a north-south latitudinal
10 transect in Alaska. *Biogeosciences Discuss.*, 11, 13251-13307, 2014.

11 Smith, L. C., Sheng, Y., and MacDonald, G. M.: A first pan-Arctic assessment of the
12 influence of glaciation, permafrost, topography and peatlands on northern hemisphere lake
13 distribution, *Permafrost and Periglacial Processes*, 18(2), 201-208, 2007.

14 Tokida, T., Miyazaki, T., and Mizoguchi, M.: Ebullition of methane from peat with falling
15 atmospheric pressure, *Geophys. Res. Lett.*, 32, L13823 10.1029/2005GL022949, 2005.

16 Varadharajan, C.: Magnitude and spatio-temporal variability of methane emissions from a
17 eutrophic freshwater lake, PhD thesis, Massachusetts Institute of Technology, Cambridge,
18 MA, 2009.

19 Walter, K. M., Zimov, S. A., Chanton, J. P., Verbyla, D., and Chapin, F. S.: Methane
20 bubbling from Siberian thaw lakes as a positive feedback to climate warming, *Nature*,
21 443(7107), 71–5, doi:10.1038/nature05040, 2006.

22 Walter, K. M., Smith, L. C., and Chapin, F. S.: Methane bubbling from northern lakes:
23 present and future contributions to the global methane budget, *Philos. Trans. A. Math. Phys.*
24 *Eng. Sci.*, 365(1856), 1657–76, doi:10.1098/rsta.2007.2036, 2007.

25 Walter, K. M., Chanton, J. P., Chapin, F. S., Schuur, E. A. G., and Zimov, S. A.: Methane
26 production and bubble emissions from arctic lakes: Isotopic implications for source pathways
27 and ages, *J. Geophys. Res.*, 113, doi:10.1029/2007JG000569, 2008a.

28 Walter, K. M., Engram, M., Duguay, C. R., Jeffries, M. O., and Chapin, F. S.: The potential
29 use of Synthetic Aperture Radar for estimating methane ebullition from Arctic lakes, *J. Am.*
30 *Water Resour. Assoc.*, 44(2), 305–315, 2008b.

Cette page ne contient aucun commentaire.

- 1 Walter Anthony, K., Vas, D. A., Brosius, L., Chapin III, F. S., and Zimov, S. A.: Estimating
2 methane emissions from northern lakes using ice- bubble surveys, *Limnol. Oceanogr.:*
3 *Methods*, 8, 592–609, 2010.
- 4 Walter Anthony, K. M., Anthony, P., Grosse, G., and Chanton, J.: Geologic methane seeps
5 along boundaries of Arctic permafrost thaw and melting glaciers, *Nat. Geosci.*, 5(6), 419–426,
6 doi:10.1038/ngeo1480, 2012.
- 7 Walter Anthony, K. M. and Anthony, P.: Constraining spatial variability of methane
8 ebullition seeps in thermokarst lakes using point process models, *J. Geophys. Res.*
9 *Biogeosciences*, 118, 1-20, doi:10.1002/jgrg.20087, 2013.
- 10 Walter Anthony, K. M., Zimov, S. A., Grosse, G., Jones, M. C., Anthony, P., Chapin III, F.
11 S., Finlay, J. C., Mack, M. C., Davydov, S., Frenzel, P., and Frohling, S.: A shift of
12 thermokarst lakes from carbon sources to sinks during the Holocene epoch, *Nature*, 511, 452-
13 456, doi: 10.1038/nature13560, 2014.
- 14 West, J. J. and Plug, L. J.: Time-dependent morphology of thaw lakes and taliks in deep and
15 shallow ground ice, *J. Geophys. Res.*, 113(F1), 1–14, doi:10.1029/2006JF000696, 2008.
- 16 Wik, M., Crill, P. M., Bastviken D., Danielsson, Å., and Norbäck, E.: Bubbles trapped in
17 arctic lake ice: Potential implications for methane emissions, *J. Geophys. Res.*, 116(G3), 1–
18 10, doi:10.1029/2011JG001761, 2011.
- 19 Tarnocai, C., Canadell, J. G., Schuur, E. A. G., Kuhry, P., Mazhitova, G., and Zimov, S.: Soil
20 organic carbon pools in the northern circumpolar permafrost region, *Global Biogeochem.*
21 *Cycles*, 23(2), 1–11, doi:10.1029/2008GB003327, 2009.
- 22 Zimov, S. A., Voropaev, Y. V., Semiletov, I. P., Davidov, S. P., Prosiannikov, S. F., Chapin
23 III, F. S., Chapin, M. C., Trumbore, S., and Tyler, S.: North Siberian Lakes: A methane
24 source fueled by Pleistocene carbon, *Science*, 277(5327), 800–802,
25 doi:10.1126/science.277.5327.800, 1997.
- 26 Zimov, S. A., Davydov, S. P., Zimova, G. M., Davydova, A. I., Schuur, E. A. G., Dutta, K.,
27 and Chapin III, F. S.: Permafrost carbon: Stock and decomposability of a globally significant
28 carbon pool, *Geophys. Res. Lett.*, 33(20), 0–4, doi:10.1029/2006GL027484, 2006.

29

30

Cette page ne contient aucun commentaire.

1 Table 1. Seep density and estimated mean whole-lake ebullition flux of Goldstream L.,
 2 Fairbanks, Alaska derived from 2011 and 2012 optical aerial image dataset and from ground
 3 surveys [Walter Anthony and Anthony, 2013; Greene et al., 2014].

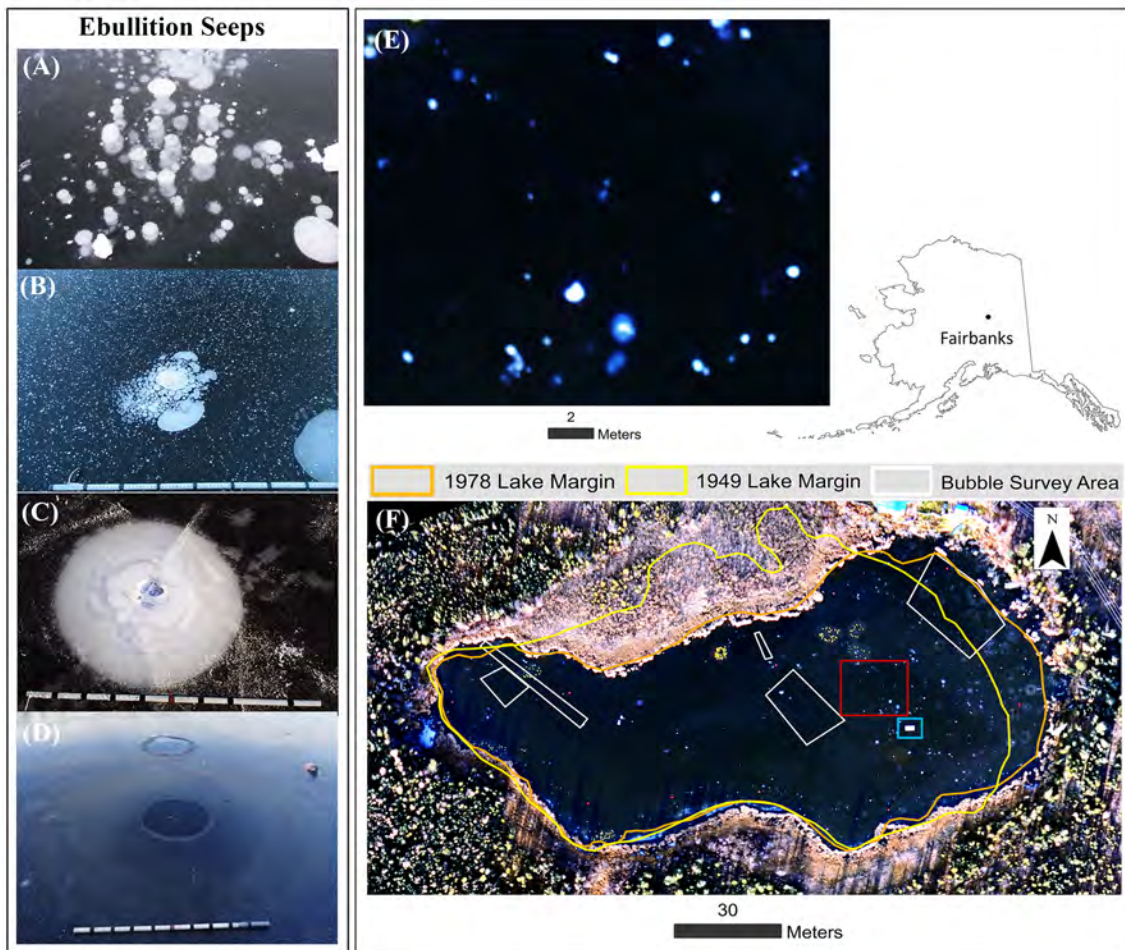
Surveys	Seep Density (seeps m ⁻²)					Mean Whole-Lake Ebullition (ml gas m ⁻² d ⁻¹)
	A	B	C	Hotspot	All Seeps	
Aerial (14-Oct-11)	0.026	0.059	0.019	0.017	0.119	174±28
Aerial (13-Oct-12)	0.061	0.083	0.021	0.021	0.185	216±33
Ground surveys	0.366	0.099	0.032	0.011	0.508	170±54

4

5 Table 2: Total number of identified bubble patches and comparison between 2011 and 2012.
 6 Patch regularity is evaluated by comparing overlap area between bubble patches mapped in
 7 2011 and 2012, assuming that overlapping patches represent the same point-source seep.
 8 Total re-appeared bubble patches (%) represent the fraction of total bubble patches mapped
 9 that are occurring in the same location in both years.

Overlapping Threshold	Year	Total mapped	Reappeared			
			Total	As one patch	In a cluster of patches	Total % reappeared
All overlapping patch	2011	1195	564	369	195	47.2 %
	2012	1860	664	369	295	35.7 %
25%	2011	1195	448	290	158	37.5 %
	2012	1860	473	290	183	25.4 %
50%	2011	1195	359	237	122	30.0 %
	2012	1860	380	237	143	20.4 %
75%	2011	1195	212	144	68	17.7 %
	2012	1860	219	144	75	11.8 %

Cette page ne contient aucun commentaire.

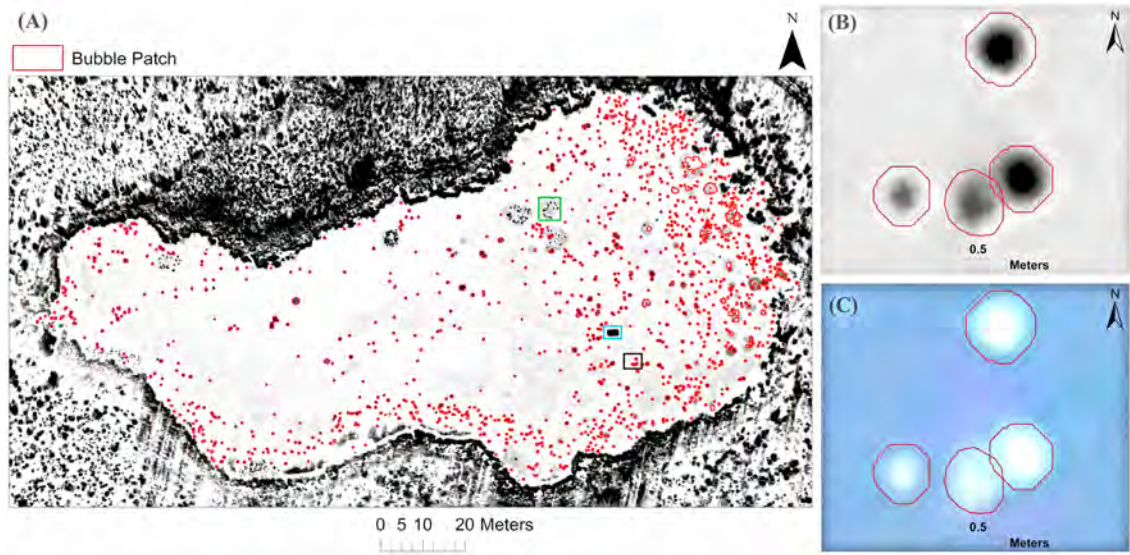


1

2 **Figure 1.** Photos showing four distinct patterns of point source ebullition seeps in early winter
 3 lake ice: (a) A-type; (b) B-type; (c) C-type; (d) Hotspot. The white speckles on the
 4 background lake ice surface in b are snow/hoar ice crystals, not bubbles; (e) A close-up (red
 5 box in the lake image shown in (f) shows the appearance of ebullition bubble patches as
 6 bright white spots on the aerial image (natural color composite of red, green and blue bands)
 7 of Goldstream Lake, Fairbanks, Alaska acquired on 14 October 2011. A rectangular wooden
 8 instrument platform (highlighted in blue box) also appears bright.

9

Cette page ne contient aucun commentaire.

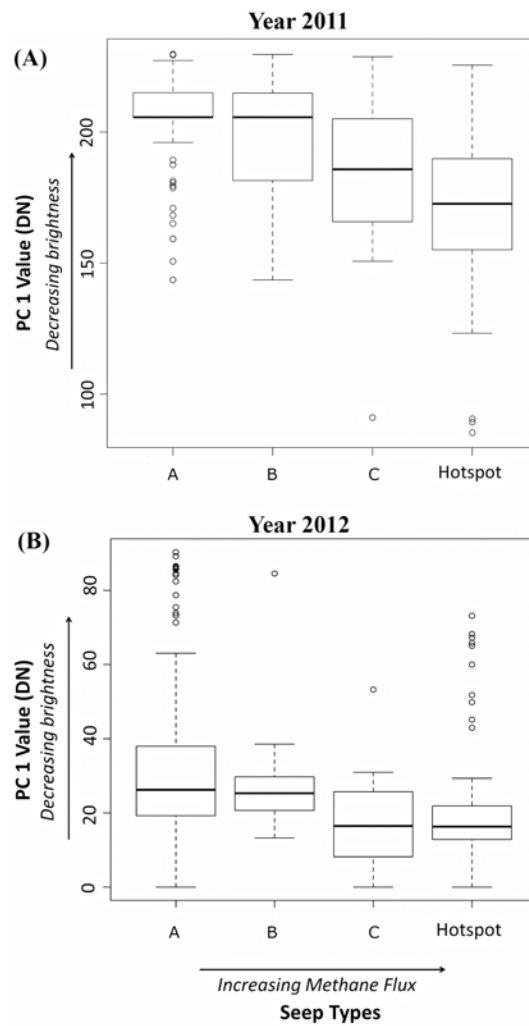


1

2 **Figure 2. (a)** 2011 bubble patch map of Goldstream L. overlaid on Principal Component 1
 3 image (PC 1); **(b)** and **(c)** show the area highlighted in the black box in **(a)** overlaid on PC 1
 4 and true color composite of red, green and blue bands (RGB) respectively. Bubble patches
 5 appear bright in RGB whereas they appear dark in PC 1. A rectangular wooden instrument
 6 platform in the center of the lake (blue box) as well as clusters of lily pads (one example
 7 highlighted in green box) on the northern and south-western parts of the lake (see Fig. 1) also
 8 appear dark on PC 1.

9

Cette page ne contient aucun commentaire.

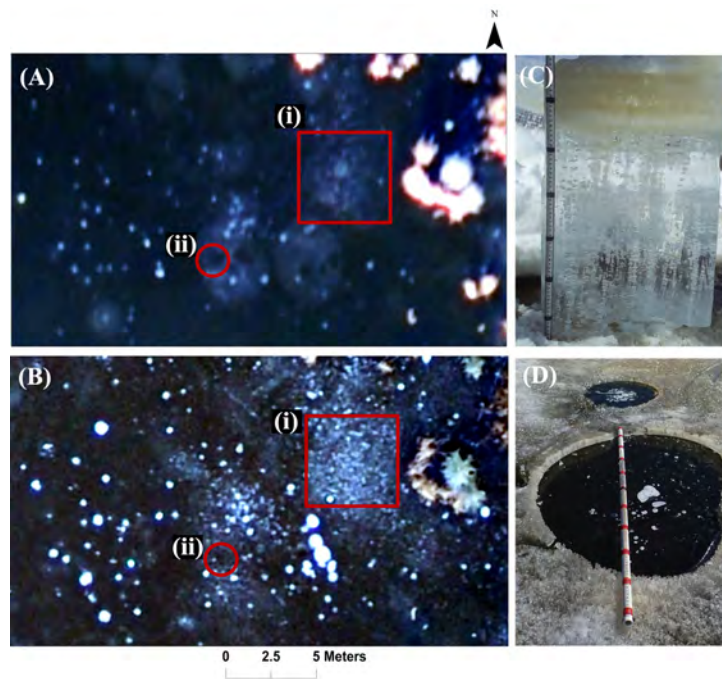


1

2 **Figure 3.** Box plots of PC 1 brightness values for bubble patches with different classes of
 3 seeps in 2011 **(a)** and 2012 **(b)**. Based on their PC1 mean brightness values, bubble patches
 4 identified in aerial images as C- and A- type seeps, Hotspot and A-type seeps, and Hotspot
 5 and B-type seeps for 2011; and C- and A- type seeps, Hotspot and A-type seeps for 2012
 6 show significant difference with p-values < 0.05 at the 95% confidence interval.

7

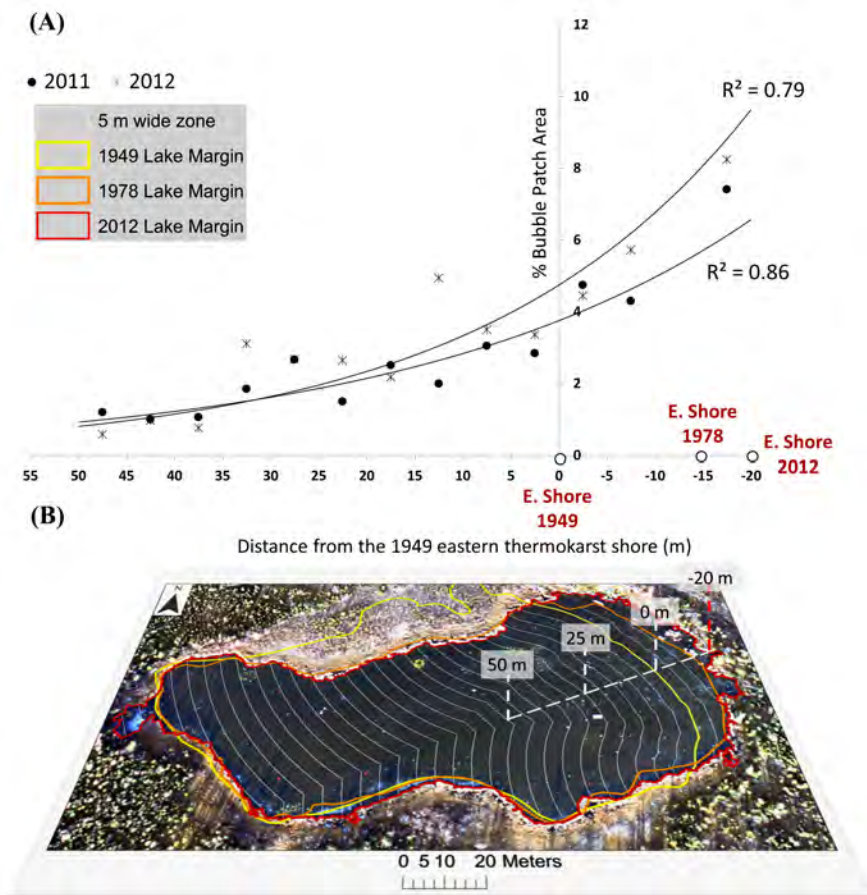
Cette page ne contient aucun commentaire.



1
2
3
4
5
6
7
8
9
10
11
12
13
14

Figure 4. (a-b) Close-up of low-altitude aerial images from Goldstream L. (~10-15 m from the eastern thermokarst margin), Fairbanks, Alaska [the same aerial extent shown in **(a)** – October 2011; **(b)** – October 2012]. The red box (i) highlights a densely packed cluster of a fifth class of seep ebullition bubbles (Tiny-type) in both years. A few B or C-type seeps also occurred among the Tiny-type ebullition bubbles inside the area marked by the red square. The red circle (ii) shows an area of Hotspots. In 2011, the Hotspots appear dark similar to clear black ice surrounded by a bright circular patch, likely hoar frost formed around open water holes; **(c)** An ice block cross-section with the Tiny-type seep bubbles in the bubble cluster area shown in area (i); **(d)** In April 2012, the Hotspot highlighted in area (ii) seem to be mostly covered with a very thin layer of fresh black ice with a few bubbles trapped beneath; however there was a mostly ice-free cavity in the ice above the Hotspots locations while the rest of the lake ice was still ~ 50 cm thick.

Cette page ne contient aucun commentaire.



1

2

3

4

5

6

7

8

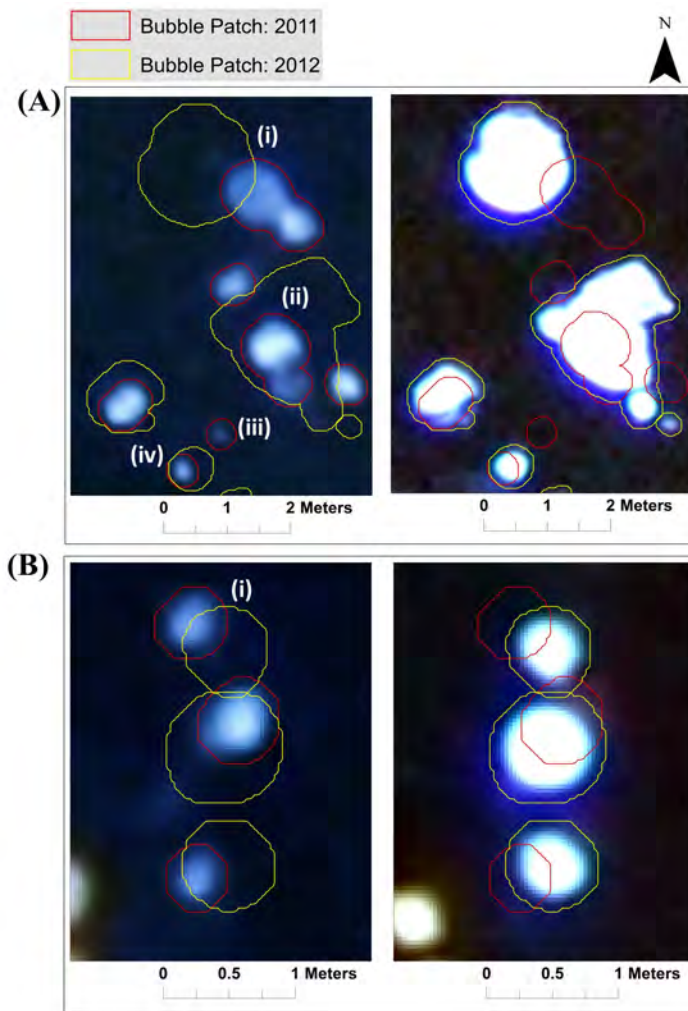
9

10

11

Figure 5. (a) An inverse exponential relationship between bubble patch percent cover and distance from the eastern thermokarst margin of Goldstream L., Fairbanks, Alaska; **(b)** The lake perimeters from 1949 (yellow shoreline), 1978 (orange) and 2012 (red) are overlaid on an aerial image acquired on 14 October 2011. Lake area change between 2011 and 2012 is minimal. The lake is divided in zones of 5 m width (white lines), for which percent bubble patch area was calculated for comparison to the distance from the rapidly expanding eastern lake margin. The vertical number marks show distance from the eastern lake margin of 1949 (marked '0 m'). The negative number indicates eastward expansion since 1949, while positive numbers indicate distance to zone westward from the 1949 eastern lake margin.

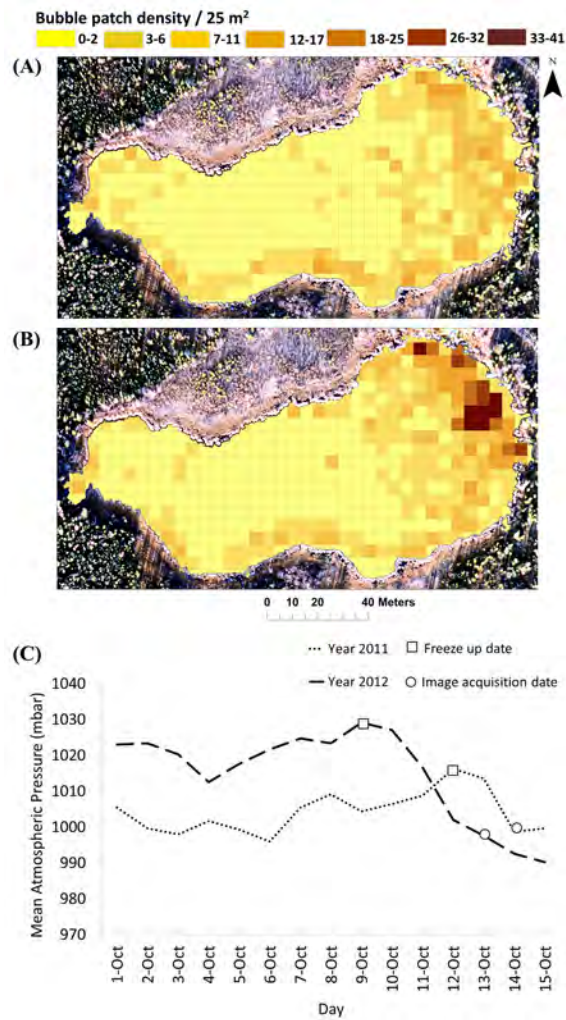
Cette page ne contient aucun commentaire.



1
 2
 3
 4
 5
 6
 7
 8
 9
 10
 11

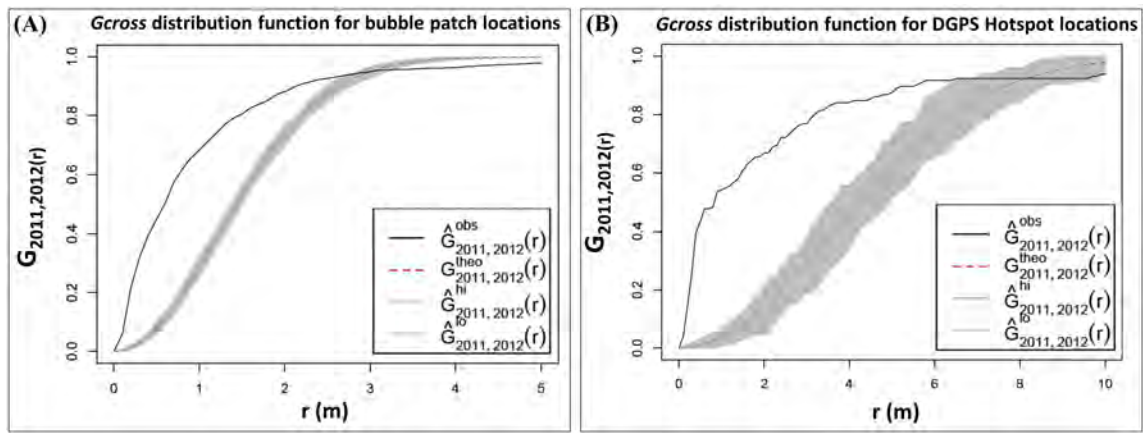
Figure 6. Comparison of bubble patches visible in thin lake ice two days after freeze-up in October 2011 (left-side images) and four days after freeze-up in October 2012 (right side images). Image pairs in a and b represent the same locations in 2011 and 2012. Four major characteristics of bubble patches are identified in panel a: (i) Bubble patches may shift up to 50 cm in location in non-consistent directions; (ii) Bubble patch size and morphology varies between years during the first few days following freeze-up; (iii) Bubble patches visible during the first few days of freeze-up in one year are not visible during the first few days of freeze-up in another year; and (iv) Bubble patches are similar in shape but not in size. Panel b shows another example of horizontal shift of bubble patches (i).

Cette page ne contient aucun commentaire.



1
 2 **Figure 7.** Bubble patch density in a 5 x 5m grid as seen in the October images of the year (a)
 3 2011; and (b) 2012. Spatial distribution of bubble patches clearly shows a higher
 4 concentration of methane emission along the rapidly expanding eastern thermokarst margin in
 5 both years; In (c) The graph of mean daily atmospheric pressure (mbar) observed between 1-
 6 15 October in 2011 and 2012 shows that the magnitude of atmospheric pressure drop prior to
 7 image acquisition was twice as high in 2012 and 2011; pressure drops are known to induce
 8 ebullition. Generally darker grid cell colors in panel suggest a higher density of seeps in 2012
 9 compared to 2011, which is consistent with (1) a two-times longer period of ice formation
 10 (four days in 2012 vs. two days in 2011) for bubbles to accumulate and (2) atmospheric
 11 pressure patterns.

Cette page ne contient aucun commentaire.



1
2
3
4
5
6
7
8
9

Figure 8. Cumulative distribution function of distances (r) between seeps identified in two different years 2011 and 2012. **(a)** Distance function for seeps derived from image dataset; **(b)** Distance function for seeps derived from DGPS field-measured Hotspots. Gray shaded area shows a theoretical seep distance function for a random seep distribution (95% confidence band). The black line shows actual observed data. The measured data indicate that a much larger proportion of the seep distances is closer than expected for a random seep distribution, suggesting statistically significant stability in seep locations over time.

Cette page ne contient aucun commentaire.

Response to reviewer # 1, D. R. MUELLER

P. R. Lindgren et al.

Comment on “Detecting methane ebullition on thermokarst lake ice using high resolution optical aerial imagery”

We are very grateful to the reviewer for giving the time to read the manuscript in detail and for providing very valuable feedback. We have revised our manuscript based on the reviewer’s comments. Below is our response to all the comments.

General comments

General comments: I am vaguely aware that some of you wrote about detecting methane ebullition from lakes using SAR. I haven’t read these papers but I see this method as being potentially complementary to optical imagery. You bring up this method in the Introduction and I kept looking for some kind of discussion of the relative merits of optical aerial image analysis and the SAR techniques examined by Engram, Walter and others (cited at the top of pg 7454). I think there is room to add this into the paper in the Discussion at least and this small touch would augment the value of this study.

This is a very good point. Thank you for the suggestion. We have now included the relative merits of optical aerial image analysis and the SAR techniques in section 5 ‘Benefits and challenges of aerial image analysis for ebullition seep mapping’. We have highlighted the limitations of SAR particularly on spatial resolution to be able to detect ebullition bubbles on small lakes and along thermokarst shoreline where ebullition is very active. High-resolution optical data can provide more realistic distribution of bubbles on the entire lake under snow free conditions and can also identify open hole Hotspots on snow covered images.

Frankly, I kept wondering how you can detect bubbles in ice with optical imagery until I realized somewhere in the middle of the Introduction that you were looking at snow free imagery. Unless you want to know about open hotspots, this to me is a constraint (well relative to SAR, I imagine). . . I think you should take care to make this clear early on in the manuscript and in the Abstract.

We have now specified the use of snow free imagery to detect bubbles in ice with optical imagery in the Abstract and the Introduction.

On pg 7452 and in several other places, you take care to mention that bubbling is highly episodic and seep bubbling rates are not constant over time. This makes me wonder about the suitability of this method in which you capture 2 to 4 days worth of ebullition and extrapolate this. Further, you check on this ‘snapshot’ with ground

Résumé des commentaires sur Microsoft Word -
Reviewer_1_Mueller_Comments_PRL_Response_BGD_092320
15.docx

Cette page ne contient aucun commentaire.

truth data taken after several weeks when the ice is safe to walk on. So a great many more bubbles ought to be present then.

We agree that since many more bubbles are present in lake ice by one to three weeks following freeze-up [time of ground surveys] compared to two to four days following freeze-up [time of aerial photos], there is the potential for the aerial survey method to underestimate the total number of seeps on the lake. That said, other factors come into play, such as hydrostatic pressure affects on bubbling rate during the 2-4 day aerial survey time frame, which can lead to some seep misclassification in the aerial photos. These factors are evaluated in Section 4.1, 4.2, 4.3 and 4.5 of the revised manuscript.

You acknowledge that the process is sporadic but don't really assess whether the method is able to capture the process sufficiently to allow for whole lake ebullition estimates. I would really like to see some further thought given. At what time scales does the bubbling vary for each type of seep? What are the implications?

Walter Anthony et al. (2010; Limnology and Oceanography Methods) provided analysis of the temporal heterogeneity of ebullition for each seep class. Large fluctuations in the daily bubbling rate are seen in the long-term bubble trap data sets for each seep class. Usually these fluctuations are related to hydrostatic pressure changes. The implications of temporally fluctuating fluxes for the seep classes are discussed in Section 4.1 of the revised manuscript.

Having said all that, all estimates of the ebullition rates seem to be fairly similar to each other (within the stated error/uncertainty of other estimates in any case). How did you arrive at these uncertainty values? How well did you do estimating the number of seeps/density of seeps for each seep type relative to the ground survey? How does this translate into how close your estimates for whole lake ebullition are? Are your aerial surveys close to the ground surveys by chance (over estimating certain types of seeps while underestimating others)? The results are in Table 1 but I think an analysis of this and the uncertainty with respect to the issues I raised above could be improved.

Standard error of mean (SEM) of each flux type estimated by Walter Anthony and Anthony (2013; JGR Biogeosciences) is the measure of uncertainty. We have stated this in the revised text. We have discussed the comparison of seep density for each seep type and total flux derived from aerial surveys relative to ground survey in section 4.3.

My last comment is an organizational one. You have 3 types of seeps initially, plus hotspots and then you add one (tiny) but don't treat it in the same way as the others. However, the hotspots should really be split into two classes based on the status of ice over top of them. I think you could improve your communication and be more organized if you thought about how and when to describe each seep type. More details are in my comments below.

Cette page ne contient aucun commentaire.

We agree that introducing the Tiny-seep class in the Methods section is confusing to the readers since very little research has been done on this seep class. Therefore, we removed Tiny-type seep from the early part of the paper and only mentioned it in the results and discussion.

To improve clarity, we have now mentioned, where appropriate, whether Hotspots were ice-free (open-hole Hotspots) or ice-covered at the time of our surveys; however based on the following two observations we did not subdivide the Hotspot class: (1) due to temporal variability in bubbling within the Hotspot class, it is possible for an ice free Hotspot to be covered by a thin layer of ice on one day and not another, and other hotspots to follow the opposite pattern depending on the recent history of their bubbling. (2) We observe ice-free cavities in spring-harvested blocks of ice from Hotspots that were originally identified as open and closed on early winter surveys.

Specific comments:

- 1. Title: Detection is one thing but I think you are doing that and more. Maybe revisit the title? I would add snow-free as a modifier of lake ice first off.**

We agree and appreciate your feedback. We have changed the title to “Detection and Spatio-Temporal Analysis of Methane Ebullition on Thermokarst Lake Ice Using High Resolution Optical Aerial Imagery”. A small portion of our study also shows the potential application of snow-covered images to identify open-hole Hotspots. Therefore, we have decided not to add ‘snow-free’ in the title.


- 2. 7451 In 25 Can you quantify dominant? What percentage of methane is released via ebullition vs other means like diffusion? Also what percentage of methane in the bubbles in this lake (or typically)?**

Greene et al. (2014; Biogeosciences Discuss.) showed that ebullition comprised 83% of total annual emissions from Goldstream Lake. The concentration of methane in Goldstream Lake's bubbles was 82-89% (Greene et al. 2014; Biogeosciences Discuss.). We have added this information in section 2 of the revised manuscript.


- 3. 7452 In 2-4 What are the implications of fast vs slow ice growth in this context? Does this alter bubble morphology and impact your bubble estimates?**

It does not have major implications in our study because we look at the very first ~ 5 to 7 cm of ice in the winter. Subsequently, winter ice growth and ebullition rate determine bubble morphology but it does not affect the estimates of our bubble surveys, as both the field data and the imagery are from very early in the season.

- 4. 7454 In 9 Geological methane seepage could be confused with Hotspots.**

 Nombre : 1 Auteur : Date : 2015-10-28 14:47:36

It is not clear what you have done about this comment in the revised ms

These are both methane sources, so that may or may not be an issue here. However, can you comment on how upwelling from springs would be interpreted? Surely this would be confused as a Hotspot using this technique. 

Geologic methane seepage and "ecological" Hotspots have in common the trait of ice-free holes in winter lake ice. They differ distinctly in associated fluxes (i.e. geologic seeps are several orders of magnitude higher flux than Hotspots) and spatial distribution. Hotspots are typically found along thermokarst margins of yedoma-type lakes and within a yedoma permafrost region they occur in nearly all lakes. In contrast, geologic ebullition seeps **are not limited to a specific permafrost type**, but can occur in any type of water body. In regions where they occur, typically those underlain by hydrocarbon reservoirs (coal, petroleum, sedimentary basins), geologic seeps nonetheless are found in only a small fraction of the water bodies. Geologic seeps are far more rare than ecological Hotspots. Also, because they have higher fluxes, the open-water holes in lake ice are usually much larger than those of ecological Hotspots. These distinguishing factors should be taken into account in analysis of open holes in remote sensing images of lake ice.

It should also be noted that ebullition associated with groundwater springs typically has a very low CH₄% (<5% CH₄) and the geologic ebullition seeps described by Walter Anthony et al. (2012; Nature Geoscience) did not include seeps associated with groundwater springs.

5. 7454 In 22 based on field-based (repetitive)

We have modified the sentence 'based on with ebullition collected data collected on the lake...'.
'


Important note: This paragraph in P 7457 now serves as a summary of our methods in the Methods section. We made this change to make it easy for the readers to get an overview of our multi-steps method before getting into details of each step.

6. 7454 In 23 – please explain why you didn't conduct fieldwork immediately after the aerial survey. (later you explain, but it would be best to comment on this right away).


We have now provided reason why we didn't conduct fieldwork immediately in this section.

Important note: This paragraph in P 7457 now serves as a summary of our methods in the Methods section. We made this change to make it easy for the readers to get an overview of our multi-steps method before getting into details of each step.

7. 7455 – It would be nice to have a location map so we can see where the lake is

 Nombre : 1 Auteur : Date : 2015-10-28 14:48:04

There seems to be 3 types of sources associated to a hole in the ice: hotspots, groundwater springs, and geologic seepage, right?
It is not clear what you have done about this comment in the revised ms.

 Nombre : 2 Auteur : Sujet : Commentaire sur le texte Date : 2015-10-28 14:49:14

Does it also imply non-yedoma lakes have no hotspots?

relative to Fairbanks or other landmarks.

The lake is located in Fairbanks. We have corrected that in the text. We have provided latitude and longitude location of the lake in section 2 and Figure 1.

- 8. 7456 ln 6 please give the number of GCPs and comment on how they were distributed across the study area.**

We have now added the details related to GCPs.

- 9. 7456 ln 9 – again, why wait so long?**

We have explained why it took long for us to do our field survey.

- 10. 7456 ln 15 – The tiny seep type really seems like an add on. Either mention this in the Introduction and follow through with it as with the other seep types or bring it up in the Discussion as a new type that was 'discovered'/characterized after this study was planned (this is what I assume happened). The Discussion is a great place to offer some insights and ponder the implications of this seep type. I don't see the middle of the Methods as an appropriate place to give background on this new seep type and start incorporating it into the manuscript.**

Yes, the presence of Tiny-type seeps and their role in altering brightness values of other seeps in the patch was discovered later in the study. We have removed Tiny-type seep from the Introduction and Method. They are only discussed in the Results and Discussion section (section 4.1).

- 11. 17457 – ln 4 delete 'are'**

'are' is deleted.

- 12. 7457 ln 16 elevations are given in m a.s.l. but you don't mention anywhere what the lake elevation is. It would be more appropriate to have the elevation in m above ground level anyway. Please consider providing this.**

We have added the lake elevation.

- 13. 7457 ln17 and 1: 17 000 for 2011 and 2012, respectively reads better.**

We have made the change.

- 14. 7458 ln 2 a second order polynomial?**

Thank you for noticing this. Yes, it is a second order polynomial. We corrected the sentence.

Cette page ne contient aucun commentaire.

15. 7459 the segmentation and classification settings/parameters are not provided. I haven't worked with eCognition but in my experience there are a myriad of settings to tweak in doing both these procedures and any of these can affect the result. What were these settings? Were the same ones used in both years? How sensitive are your results to changes in these settings? How do we know you optimized this step? Please provide details on this.

We appreciate your comments. These are some crucial technical questions. Yes, there are number of settings in eCognition that can affect the result (please see reply #17 below). The procedures we used are same in both years except the threshold values applied in some of these ruleset settings are different. This is just because image quality varies depending on the prevailing conditions during image acquisitions. Therefore, threshold used in one image band to identify some object may not be the same between years. We have explained the object hierarchy and general rule applied to map bubble patches in both years in the paper (section 3.3.2 and supplementary section in the new version of manuscript). Please see some examples on how we set rules in reply #17.

This paper is focused on the analysis of ebullition dynamics using information derived from optical images. Therefore, we have only provided a general overview of the mapping technique. We realized that having technical details as well as the analysis section in one paper was going to be way too much information for readers. Many readers may find this complicated. A technical paper on methane ebullition bubble mapping using Object Based Image Analysis (OBIA), which provides all the details, is in preparation for peer-reviewed publication. We have cited the paper in prep. in this section of the manuscript to guide the readers if they are interested to learn more about the technical details of the methods.

Please note that we also decided to move some portions of methods in section 3.3 in the revised manuscript to the supplementary section, as our method section was long and difficult to follow for other readers. We have now provided details on Principal Component Analysis (PCA), object-based segmentation and classification, and classification of bubble patches as supplemental text. This has helped to keep the method description simple and straightforward in the main paper. To improve the clarity, we also sub-divided sections of methods in the revised manuscript. Please see the replies, #24 and #25, below.

16. 7459 why did you segment and classify the land cover as well as the lake? Would it not be simpler to mask out the land first and study only the lake area?

In the OBIA technique (or in eCognition) segmentation is always the first step. So, even to mask out the land first, the image has to be segmented and then classified to separate land from lake to study only the lake (which is the first stage

Cette page ne contient aucun commentaire.

in our classification). Also, we used winter images for classification; hence it is less straightforward to have a land-lake (water) classification as first step. One of the options could have been manually mask out the land and only work on the lake part. But one of our goals was to develop a semi-automatic ruleset in eCognition to create transferable and efficient steps to study multiple lakes. And this current method is capable of separating land from frozen lakes with few manual inputs. The manual input would be to assign a correct threshold on the setting if needed.

17. 7460 I assume that this step is, technically-speaking, an unsupervised classification but perhaps not? Can you please clarify? What are we to make of the 98% accuracy? This seems to reflect how well your customization of the eCognition routines worked on the image(s) you worked with. Since you didn't use an independent dataset to validate the classification routine, I don't see this as a true validation accuracy. That's ok, but please make this clear.

Yes, technically speaking traditional supervised classification requires training dataset and we do not use that, so in that sense this could be an unsupervised classification but still it is not a completely unsupervised classification. We make rules by defining thresholds on variables such as image bands, object's relation to neighbors etc. to classify image objects. For example, we set a threshold on PC 2 brightness component to separate lily pads from lake ice. We use a threshold on PC 1 component to separate dark and white ice on the lake. We use morphological filter to identify bubble edges for which we use PC 1 component. We also define rules based on object's neighbor's relationship. These are just a few examples. There are many different rules and the classification is narrowed down to the lowest level to identify bubble patches. Therefore, it is correct that the accuracy reflects how well our customization of the eCognition routines worked on the image.

Due to thin lake ice condition on image acquisition days, it was not feasible to collect ground truth data of ebullition bubble patches for the purpose of accuracy assessment. We manually classified bubble patches on the image to use them as validation sites. We did not check our classification accuracy in terms of object's geometry or boundary delineation. We only performed quantitative site-specific accuracy assessment using error matrix that only checks the agreement of object classes between manually classified reference sample and object-based classification results. We have provided more details on accuracy assessment in the revised manuscript as a supplemental material to keep the paper concise.

18. 7460 as above, please explain a bit more on how you selected the threshold (what was the threshold ultimately?)

The threshold was a DN value on image bands, an input for contrast split algorithm, that separated open-hole Hotspots from the snow-covered lake. We

Cette page ne contient aucun commentaire.

have now provided this information. We have provided reference for contrast and split algorithm in eCognition for more information.

- 19. 7460 ln17 It is fairly confusing to the casual reader that dark pixels are bubbles and light pixels are ice in the PC1 variable. I would suggest that you arrange for this to be the reverse, which is more intuitive. You could insert a step here 'the value of PC1 was multiplied by -1 [and offset by ##?] to reverse this band, making bubbles patches . . . ' I don't believe this will influence any subsequent results, but please check. Alternatively, you could just display the PC1 results in reverse and explain this in the figure caption.**

Thank you for your suggestion. We agree that the way PC 1 variable is related to the bubble brightness in the paper is not very intuitive. We have now reversed the PC 1 values (i.e. dark pixels/low DN values in PC 1 component is less bright bubbles and bright pixels/high DN values is brighter bubbles). Yes, this does not influence any subsequent results. We have explained inverted PC 1 in section 3.4.1 and more detail is provided in the supplemental text.

- 20. 7460 ln 22-3 We applied a post-hoc Tukey's Honest Significant Difference test . . . identify significantly distinct seep types. Also elsewhere you have 'Honestly' as well.**

We changed the sentence to “We applied a post-hoc Tukey's Honestly Significant Difference (HSD) test, if the null hypothesis was rejected, to identify significantly distinct seeps.”

- 21. 7461 ln 4 explain more on the MLC classification. What is the number of training samples? Were any samples taken for validation (at a different end of the lake)? What thresholding options and other parameters did you use?**

We have added more details in section 3.4.2 regarding the number samples for training MLC and validating the MLC results. Most of the samples are concentrated along the thermokarst margin of the lake. But we do have other randomly distributed samples from all other parts of the lake where bubble patches are visible.

The MLC classification only uses spectral characteristics derived from all visible bands (RGB) and PC 1 component of these bands of the training samples we provided. We have stated this in section 3.4.2.

- 22. 7461 ln 8 integrating size as an additional feature – again, details are lacking. is this a step after the MLC? How did you do this?**

Yes, there is another step after the MLC. The MLC categorized bubble patches solely based on pixel spectral characteristics i.e. only included brightness parameter derived from the training samples. MLC was a pixel-based

Cette page ne contient aucun commentaire.

classification; therefore a segment of bubble patch had more than one class of seep assigned depending on the variation in brightness of the pixels within the patch. Since the size of bubble patches is also an additional important indicator of seep class and methane flux (Walter Anthony et al., 2010; Limnology and Oceanography Methods), in the next step we further investigated the size of each seep class in a bubble patch identified by MLC. Based on the size information and combination of seep classes in a patch, we then re-assigned bubble patches to a more accurate methane flux. We have added more details in the supplementary section of the revised manuscript (Supplementary Text S3 and Table S1 in the revised manuscript).

23. 7461 ln 12 seep types - add s

‘s’ is added.

24. 7461 ln 14 We studied - remove ‘further’

We removed ‘further’. This is a separate subsection now in the revised manuscript (Section 3.4.3).

25. 7461 ln 21 Finally we evaluated. . .

We removed ‘Finally’. This is a separate subsection now in the revised manuscript (Section 3.4.4).

26. 7461 ln 27 – I would suggest that you not capitalize Complete Spatial Randomness and make this into an acronym. Spatial randomness is an easy concept to understand and by making it into an acronym, I was mistakenly thinking this was a procedure you applied. It slowed me down in this section. As well, you need to highlight in the part of your explanation that your null hypothesis is ultimately that the difference in spatial patterns are random, not that the spatial patterns themselves are random. This is important as your seeps predominate in certain parts of the lake.

Complete spatial randomness is in lower cases and removed the acronym.

We agree that the null hypothesis is confusing in the manuscript. We have revised the text to highlight that our null hypothesis is ultimately the difference in spatial patterns are random.

27. 7463 ln 5 – I would start this section a little more gently than getting into PCA results and correlations. How many seeps of each type were there? Did this change from year to year?

We have now described PC 1 brightness characteristics of each seep type at the beginning of section 4.1. We have also shown number of samples (number of

Cette page ne contient aucun commentaire.

seeps we used to compare field-based flux with aerial survey) and PC 1 brightness mean±standard deviation of each seep type in Figure 3 in the revised manuscript. Yes, the number of seeps of each type used for comparison changed. This is just because 2011 had less number of bubble patches mapped compared to 2012.

28. 7463 ln 6 neg correlation – can you give more detail on this? It seems like there might be more to say. . .

We have rearranged the sentences to make it clear.

29. 7463 ln 7 – were assumptions for the ANOVA met? I see the ANOVA in supplementary material. Make it clear that hotspots are ice covered.

We have now made it clear that Hotspots are ice covered.

30. 7463 ln 10 and 11 – writing significantly, $p < 0.05$ and 95% confidence interval is redundant. Chose one of these.

Thank you for noticing this. We are only using $p < 0.05$ in the revised manuscript.

31. 7463 ln11 to 14 – can we have more descriptive results on PC1? What is the range of bubble values in PC1? What is the range of lake ice (congelation and snow ice), snow, open water. . . lily pads, etc.

More detail regarding the PC 1 values of different image objects is discussed in the technical paper (in prep.). The PC band value range of lake, snow, open water etc. varies between years. Please see reply #15 above. In the revised manuscript, we have reported the results on PC 1 values (mean and standard deviation) of each bubble seep type in section 4.1 and Figure 3.

32. 7463 ln 13 less bright ==> darker

We have replaced 'less bright' with 'darker'.

33. 7463 ln 18 given th spatial resolution

We corrected this line.

34. 7463 ln 27 – it might be worth considering two subclasses of Hotspot for practical/logistical purposes throughout your paper – Ice covered Hotspots and open Hotspots (use your own terms, by all means). This distinction, once made clear early on, could then help you out here and elsewhere when you need to separate these two manifestations of hotspots. For instance your ANOVA is for ice-covered Hotspots only and seeking open hotspots is the sole purpose of the snow covered lake imagery, etc.

Cette page ne contient aucun commentaire.

Thank you for your suggestion. We have made it clear what we are looking at on the images whether ice-covered or open-hole Hotspots in section 3. We also made it clear early in the Methods section 3.1 that ice-covered ebullition seeps (A, B, C and ice-covered Hotspots) are referred to as ebullition bubble patches and we are using snow covered lake imagery to map open-hole Hotspot locations. Please see our reply in general comments above regarding ice-covered vs. open-hole Hotspots.

35. 7465 ln 1-4 You made a big, late-breaking introduction of the fifth class of seep in the Methods and now we find that it cannot really be distinguished. I would suggest that you consider the place that Tiny-type seeps occupy in this paper (see my comment above). Depending on your decision here, you might consider adding Tiny type to a boxplot.

We have removed the discussion of Tiny-type seep from the Methods and only mentioned it in the Discussion. Please see our replies related to Tiny-seep above in general comments.

36. 7465 ln 6-7 awkward sentence

We have changed the sentence structure to make it clear.

37. 7465 ln 10 – it would be nice to have a table for the users and producers accuracy

Accuracy table is now provided as a supplementary material.

38. 7465 ln 11 – mostly arising from

We replaced ‘rising’ with ‘arising’.

**39. 7465 ln 19 – aha, here we find out what took you so long to get out there ;-)
Good reason, of course, but please write this in the Methods. I am sure we can all agree it is best not to have a delay between the imaging and the ground truth. Also, if seeps are sporadic, you are not integrating over much time (only 4 days). Longer would be better. How can this be mitigated – why not discuss this? I realize it could snow any time so you are probably wanting to get data right away after freeze up. . . . what about repeat surveys every 2nd day until the ice is safe to walk on? That way you can use the last possible date for study. One last question, when you did finally get onto the lake, was it snow-free?**

We have now provided the reason for a gap between image acquisition and fieldwork early in the Methods. We agree that repeated survey is an option to mitigate this issue but may not be very cost efficient. Also, it is very rare that snow free condition will prevail until the ice is safe to walk on for ground

Cette page ne contient aucun commentaire.

surveys. We have stated this issue in section 5.

40. 7466 ln 3 could you say reductions instead of changes?

We added 'dynamics' after 'ebullition' in the current sentence: **It is well established that ebullition dynamics are inversely related to changes in barometric pressure** (Mattson and Likens, 1990; Fechner-Levy and Hemond, 1996; Scandella et al., 2011).' This is more accurate. A rise in pressure suppresses ebullition, while a drop in pressure enhances ebullition. So, pressure changes in both directions have differing affects on ebullition

41. 7466 ln 20 field-based = when exactly?

The results are from the observations over multiple. We have now made it clear.

42. 7469 ln 3 – can you just mention this was due to a different atm pressure, just to be clear?

We have now mentioned it.

43. 7471 – here is a good place for a longer discussion on SAR vs optical for your application.

We have now added the discussion on SAR vs. optical in section 5. Please see our reply in general comments.

44. 7471 ln 22-27 – these are crucial points/limitations and should be also mentioned in your Abstract and Conclusion

We have mentioned these limitations in the Abstract and Conclusion.

45. 7472 ln 1 allow to map – awkward/unclear

We corrected this line.


46. 7472 ln 4 – bubble patch brightness, with some confusion.

We replaced brightness with 'PC 1 brightness values'.

47. 7472 ln 5 – remove 'understandable'

We removed 'understandable'.

48. 7472 ln 10 – results also imply the potential, given the caveats raised above, to apply...

 Nombre : 1 Auteur : Sujet : Commentaire sur le texte Date : 2015-10-28 14:50:25

I think inversely needs to be removed to clarify the sentence

We corrected the line.

- 49. 7473 – this section reads like a summary, can you bring your findings and their significance together and draw some more conclusions instead of recapping the Results?**

Thank you for your suggestion. We have shortened the Conclusion and only highlighted the major findings and their implications.

- 50. 7473 ln 12 – can you correct for, or account for, the difference in pressure? Or at least propose a way to do this in the Discussion? Seems like it might be possible.**

[1]We haven't yet looked into this correction in detail. But we agree by using multi-temporal imagery (several years of data) this could be possible.

- 51. 7481 In the table, can you put two lines for the ground surveys – one for 2011 and another for 2012? Or if they only happened once, put the year.**

The ground flux estimate is based on multiple year data. We have stated that in the manuscript in section 4.2.

- 52. 7482 Is there a better way to lay out this table? It seems busy and isn't very intuitive. . . I don't have a suggestion right now, sorry.**

We have removed the table since the results are already explained in the text. We felt that the information is redundant and the table is confusing. Removing the table also helps to make the manuscript more concise

- 53. 7483 Nice to have the map of Alaska but it would be nice to have a zoomed in study site map of the lake and surrounding area. You can use this to display ground truth sites and other info that is missing from your current figures.**

Please see reply # 7. We have displayed ground truth sites (surveyed polygons) on the figure. We have explained important characteristics of the surrounding area in the Study Area as well that we think can help readers to get an idea about the surrounding.

- 54. 7484 I think lily pads should be brought up elsewhere in the manuscript – for example, how can these be distinguished from other classes in PC1 or otherwise?**

We used PC 2 band to distinguish lily pads from lake ice since vegetation had distinct characteristics (very low PC 2 values compared to lake ice). We briefly mentioned that we also used PC 2 bands to classify image objects in the paper (now in supplementary section of the revised manuscript). Please see reply # 15

and # 17 above. The details regarding techniques on identification of bubble patches are discussed in the technical paper (in prep.).

55. 7485 with p values < 0.05 as determined by Tukey's. . .

'by Tukey's HSD test' is now added to the sentence.

56. 7487 Fig 5a. Can you write out these empirical relationships? What about the p value of these relationships and the RMSE of your prediction? Also, I am having trouble understanding how the x values you have on the abscissa can produce the curves you drew in an exponential relationship!?

Thank you for the suggestion. We have now added regression equations, p-value and standard errors in the figure. We understand the confusion on the x-axis values and exponential relationship. We had the distances from the 1949 eastern lake margin to illustrate high methane bubble concentration along the thermokarst margin. We have replaced the graph with distances from the modern lake thermokarst margin (2012 thermokarst margin). The exponential relationship is between the distance from 2012 margin and the bubble patch percent coverage. We have marked where 1949 and 1978 thermokarst margins existed in relation to the modern margin in the graph.

57. I wonder if it is possible to relate to ebullition rate as opposed to the area of the patches? I acknowledge it is a stretch but you might consider doing this perhaps in addition to the area (on a separate y axis?).

We appreciate your suggestion but for now we would like to keep the relationship as it is since the observations are made during the two very short windows of time 2–4 days after freeze-up. Relating distance from the thermokarst margin to bubble patch area is the most direct and accurate representation of our observations.

58. 7487 Fig 5b. Please remove the perspective view of the lake. This adds nothing and makes it more confusing to understand. Can you explain why the N shore has changed? Is this infill?

Thank you for your feedback. We have now removed the perspective view of the lake.

We suspect that the lake either partially drained or that the water level decreased sometime after 1949, though we have insufficient information to explain the cause for the observed change in lake shape along the north shore between 1949 and 1978.

59. 7488 I think you should calculate your potential geolocation error and declare it here and where you look for spatial randomness in the text as well. Also, is it possible to look at whether the seep type changes year over year

Cette page ne contient aucun commentaire.

with your methods? (ie., not only the position. . .). Perhaps you can comment on that in the Discussion as this might be an interesting thing to do someday.

We appreciate your comment. We understand that geolocation error is important. Since our geo-location error was not that significant (on average < 20 cm) in our analysis, we didn't mention it in the paper. Now we have declared it section 4.5 and Figure 6.

It is challenging to look at whether the seep type changes with only two-year dataset. However, with many years of data it could be possible to check how bubble patches change (by comparing brightness and size) to analyze possible seep type changes. We have highlighted this possibility in section 4.5.

60. 7490 Remove the legend from the graph. It is not required if you put this info in the caption. Explain the significance of where the black line crosses the shaded area, does that mean the process is random at that length scale? What does being on the other side of the curve mean?

The legend has been removed. As suggested we have provided the meaning and shape of the curves and other details in the caption.

Cette page ne contient aucun commentaire.